

Savings and Migration in a Warming World*

Alexander C. Abajian[†]

Please use the link on my webpage [[here](#)] for the latest version.

November 27, 2024

Abstract

This paper introduces a global model of climate change where agents can adapt through precautionary savings and migration. Analytical results show how the extent to which migration will serve as adaptation, and in turn alter the global population distribution, will be determined by mobility costs. Adaptation through migration is income-dependent; while wealthy agents are able to pay international migration costs in order to take advantage of locations forecast to gain under climate change, poor and low-wealth agents are unable to move and can only insure against adverse shocks through savings. The calibrated model predicts that 6 percent of the global population will migrate internationally because of climate change by the end of the 21st century. Welfare effects from climate change are highly unequal; warming under RCP4.5 raises the wealthiest agents' welfare by 4.0 percent, while the poorest agents in low-income countries experience losses of 8.5 percent.

Keywords: Climate change, international migration, incomplete markets

JEL Classification: D52, F22, J61, Q54

*I am deeply grateful for continued encouragement and guidance from my advisor Javier Birchall, without whom this work would be preliminary at best. This paper was improved substantially by feedback from Kyle Meng, Peter Rupert, Nick Pretnar, Yueyuan Ma, Tamma Carleton, Kieran Walsh, Lint Barrage, Ishan Nath, Greg Casey, Jesús Fernández-Villaverde, John Stachurski, Fedor Iskhakov, Paulina Oliva, and Per Krusell during my time at U.C. Santa Barbara. I owe special thanks to Yang Gao, Yuanzhe Liu, Thomas Fullagar, and Sabrina Berger for continued support in the macroeconomics group and in the Ph.D. program more generally. All errors are my own.

[†]Economics Ph.D. candidate at University of California, Santa Barbara. Email address: alexander_abajian@ucsb.edu.

1 Introduction

Climate change due to anthropogenic greenhouse gas (GHG) emissions will substantially alter the spatial distribution of people and economic activity over the coming century. A broad literature has established that climate change will affect output and investment (Yang 2023; Nath, Ramey, and Klenow 2023) as well as location choices (Hoffmann et al. 2020; Liu, Shamdasani, and Taraz 2023). The resulting shift in populations towards less-affected places will be governed by how adaptation – individuals’ behavioral adjustments which take future warming as given – will manifest through both relocation of people across space as well as resources over time (Desmet and Rossi-Hansberg 2024). The amount each adaptation channel – precautionary savings and migration – will be put in use across the globe depends on both the local efficacy of each channel as well as the extent to which either is at all accessible. Existing climate macroeconomics literature incorporating multiple regions studies how each of these channels, in isolation, will allow for adaptation.

This paper focuses on how the global population will adapt to the spatially-differentiated effects of climate change given the ability both to migrate towards better-off locations and partially insure through precautionary savings. Including both margins draws a connection between two leading modeling paradigms in the multi-region climate macroeconomics literature — neoclassical and spatial — which have focused on how either local capital accumulation or migration will, in isolation, allow people to respond to climate change.¹ The neoclassical integrated assessment model (IAM) paradigm views adaptation to climate change through the lens of a consumption-savings problem, where the differentiated effects of climate change across space affect the allocation of local resources over time (Krusell and Smith 2022). While this approach is useful for characterizing how climate change affects adaptation through capital accumulation in locations around the globe (e.g., through building seawalls, improving irrigation systems, or installing air conditioning units), it foregoes modeling migration decisions.² The latter spatial integrated assessment model (SIAM) paradigm draws on the economic geography literature, abstracting from intertemporal savings and capital accumulation in favor of characterizing how migration, trade, and local sectoral compositions shape adaptation to climate change (Cruz and Rossi-Hansberg 2023; Cruz 2023).

Towards integrating these two paradigms, I present a macroeconomic model of global

¹I delineate these differences in Section 1.2.

²A notable exception to this is Alsina-Pujols (2021) who examines how climate change will affect migration in the form of international refugee flows between the global North and South. Alsina-Pujols (2021) shows that Northern countries have in the past displayed limited willingness to accept refugees from the global South and tend to experience political backlash in the aftermath. This channel increases Northern countries’ willingness to pay for climate change mitigation as it also decreases Southern emigration.

climate change that retains the intertemporal choices of the neoclassical formulation while allowing for agents to adapt to climate change through migrating across space. The central mechanism that differentiates my model from prior work is that explicit financial costs of international migration can preclude movement entirely for the poorest individuals. While migration in the calibrated model would be beneficial for many households in terms of gains in real income, credit constraints may prevent them from being able to do so. This aspect of the model reflects a large body of literature which finds that international migration is increasing in income at low income levels where liquidity constraints play a critical role in preventing the poorest agents from moving (Cai et al. 2016; Bazzi 2017; Cai 2020; Barbosa Alves and Braulio 2023).

The paper begins with a two-period model where agents can both migrate and save in order to adapt to a changing climate. Limiting cases nest stylized versions of the neoclassical and economic geography models of global warming, namely when either migration costs are preclusively high or the returns to savings are zero. In partial equilibrium, comparative statics align with intuition: emigration declines with migration costs, increases with local climate damages, and may be precluded entirely by liquidity constraints. Adding a savings channel to the conventional spatial framework leads to all regions retaining a nonzero share of agents. This emergence of “always-stayers” under savings occurs regardless of the size of local losses from climate change; unless losses from a decision are infinite, the class of models that use unbounded taste shocks for tractability will always have agents for whom it’s optimal to stay in place when they can guarantee some future income. In general equilibrium, the final distribution of modeled agents depends on the relationship between migration costs and future productivity levels across space. Identifying whether migration or savings will be more beneficial or widely-used as adaptation requires fully-characterizing the distribution of migration costs, baseline productivity levels, and effects of climate change.

The full model takes these ideas to a calibrated infinite-horizon incomplete markets model where a continuum of agents is divided across regions around the globe. Each period, agents solve a traditional consumption-savings problem in addition to a discrete decision over whether and where to move. Modeled countries differ in fundamental productivity levels, migration costs, and initial temperature levels. Agents in each region face idiosyncratic labor supply risk which leads to precautionary savings (as in Aiyagari 1994) and induces a rich cross-sectional distribution of wealth within and across countries. Unlike in other spatial frameworks (c.f. Cruz and Rossi-Hansberg 2023), migration costs enter the model as financial costs rather than pure disutility. Whether it is visa fees, transportation costs alone, or “golden passports”, this aspect reflects the reality that migration is never entirely free of charge (Recchi et al. 2021; Surak 2021). Real costs of movement interact with borrowing

constraints such that poor agents must self-finance international migration. This channel also allows idiosyncratic income shocks to affect migration decisions; while the relative wage of outside locations determines their value as insurance against future climate change, negative income shocks can (depending on local migration costs) preclude leaving (Bazzi 2017; Cai 2020). The combination of these features yields an environment where climate change affects both local income levels as well as migration decisions differently for poor and rich agents in each country.

1.1 Main Findings

I calibrate migration costs in the model using the method of simulated moments to minimize the distance between equilibrium country-level population shares predicted by the model and observed average shares for the period of 2010-14. The calibrated model can explain 75% of the variation in observed population shares in the data across the 154 countries in the model. Calibrated values for existing barriers to movement between countries – the real costs of international migration that minimize the distance between data and modeled moments – are substantially larger than annual wages for a qualitatively important share of agents. When translated to real world terms, these costs are in the thousands of U.S. dollars, values in-line with estimates of barriers to movement from the empirical migration literature (Clemens, Montenegro, and Pritchett 2019).

I use the calibrated model to perform counterfactual steady-state and transition path experiments that forecast how climate change in the 21st century will affect the global population distribution. The projected aggregate shocks from climate change driving the model are based on two benchmark scenarios for global GHG emissions, Representative Concentration Pathways (RCP) 4.5 and 8.5. I use grid-cell level temperature projections from the Coupled Model Intercomparison Project Phase 6 (CMIP6 – Eyring et al. 2016) to map each RCP into time series for annual changes in country-level average temperatures relative to initial conditions in the modeled 2010-14 period. I combine these country-specific temperature forecasts with base-temperature specific damages functions estimated by Nath, Ramey, and Klenow (2023), henceforth NRK, to create forecasts for how climate change will affect productivity growth through 2100. These two inputs combine to yield RCP-specific changes in annual productivity growth for the entire transition period, which drive how agents' behave as the world moves towards a new (warmer) equilibrium .

Under the mean forecast of temperatures from CMIP6 for RCP4.5, population-weighted average temperatures rise by 2.0 degrees Celsius globally relative to the 2010-14 period. When this warming is translated into global changes in productivity using the estimates from

NRK, RCP4.5 causes an 8 percentage point decline in cumulative aggregate productivity growth in 2100. Warming is far from uniform geographically. Global population centers in South and East Asia experience increases between 1.5 and 2.0 °C, while parts of Northern Europe and Scandinavia warm by over 3 °C. Dispersion in warming in combination with baseline heterogeneity in average temperatures induces a huge gradient in the productivity effects of climate change; while warm countries lose 20 percentage points of growth by 2100, the coldest countries experience additional productivity growth of 50 percentage points.

The global gradient of productivity changes induced by warming under RCP4.5 substantially shifts the new steady-state distribution of people across the world. Twelve percent of the world population relocate (on net) to different countries after the cumulative effects of warming through 2100 are fully realized. In contrast to prevailing narratives suggesting that huge waves of emigration will take place in the global south (Vince 2022), migration is most-concentrated among rich countries. Forecast changes in populations in Sub-Saharan Africa, a region where both baseline productivities are relatively low and the impacts of climate change are forecast to be very negative, are all lower than 0.1 percent of the global population. This is not a result of low overall rates of migration; many agents do migrate each period and the poorest agents are those who would otherwise gain the most. Instead, the high cost of international migration and limits on borrowing preclude the poorest agents from migrating even when they know they will face large declines in future real income. The largest population declines in the baseline model occur instead in the United States, Australia, Japan, and Western Europe. These declines are not due to the direct local effects of climate change on productivity in these countries, but rather because rich agents there have sufficient income vis-à-vis migration costs such that they can take advantage of colder locations forecast to experience future productivity gains.

The next portion of the baseline experiment uses transition path methods to simulate the full series of macroeconomic dynamics under RCP4.5. Almost 6 percent of the global population (approximately 400 million people) migrate internationally on net in response to climate change within the 21st century. Like in other models (Bilal and Rossi-Hansberg 2023), anticipation effects prove important for determining population dynamics when agents have rational expectations over the damages from climate change. On aggregate, the welfare losses from climate change are almost zero; adaptation through migration proves to effective insurance (and indeed can provide gains) for agents who can move to cooler countries that become more productive. However, this small aggregate effect masks a highly unequal distribution of gains and losses at the individual level. A warmer world leads to welfare losses as high as 8.5 percent for poor agents in low income countries, as these agents are unable to afford to migrate and are in places that are worst-hit by climate change. In contrast, rich

agents who are not constrained can freely migrate to countries where productivity rises and experience welfare gains as large as 4 percent. On the whole, results from the transition path add to the growing body of research that suggests the welfare effects of climate change will be highly unequal both by geography as well as across income groups within a given country.

The divergence in behavior between poor and rich agents becomes extreme when the counterfactuals are recalculated under the larger productivity changes due to RCP8.5 or when in addition to the warming under RCP4.5, migration costs are doubled. Population changes under RCP8.5 (roughly 4.2 °C warming and 17 percentage points of productivity growth loss globally) are qualitatively similar in terms of where populations rise and fall relative to benchmark case, albeit much more extreme in magnitude. Over 20 percent of the global population migrates internationally, with increases in population levels most-concentrated in the coldest countries today, which experience the largest productivity gains from climate change. The model is sensitive enough to migration costs that the distribution of agents across space becomes close to a degenerate one under the scenario where, in addition to the warming under RCP4.5 migration costs are doubled. Modeled agents' fall into one of two equilibrium behaviors: poor agents around the equator become stuck almost entirely in their countries or regions of origin, while nearly all rich agents make it to one of the countries where real wages rise due to warming and then stay put because emigration due to idiosyncratic shocks rarely outweighs the costs of moving after they are doubled.

The broad prediction of both the simple and calibrated models presented here is that the value of migration as adaptation will depend on the *financial* costs of migration in addition to any utility costs. When existing spatial approaches are modified to account for the nonlinearities that emerge when migration is not free of cost, forecast patterns of adaptation to climate change diverge substantially from what would otherwise be predicted by the effects on the global productivity gradient alone. This feature of the model illustrates the crucial role of how barriers to migration may lead to nonlinearities in the realized migration patterns over the coming century. The resulting uneven uptake of migration across income and wealth levels drives the results here to diverge from those of existing SIAM frameworks examining climate change (Cruz and Rossi-Hansberg 2023; Cruz 2023). The ability to pay whatever the costs of international migration are in the coming century will play a non-negligible role in shaping what the world looks like as it warms and pressures on emigration build, and will distinguish between who we will observe moving as opposed to who would move if it were feasible.

1.2 Related Literature

Neoclassical models: Neoclassical models of climate change with multiple regions (e.g., Nordhaus and Yang 1996; Nordhaus 2010; Krusell and Smith 2022; Yang 2023) typically build on the Dynamic Integrated Climate Economy (DICE) model framework (Nordhaus 1992). These models augment the Ramsey model of optimal savings to account for how greenhouse gas emissions from production as well as mitigation efforts and abatement affect welfare and the climate globally (Barrage and Nordhaus 2024). Agents across a set of (potentially many) regions solve representative agent problems in autarky facing a global externality in the form of climate change due to emissions from energy use. The optimal response for a policymaker in the decentralized setting is to adjust energy use in each region to lower emissions through the use of Pigouvian taxes. The current version of DICE that allows for multiple regions (Yang 2023) and the state-of-the-art multi-region neoclassical IAM in terms of granularity (Krusell and Smith 2022) serve as preeminent guides for “place-based” policy in a world where space is relevant only in determining how climate change affects productivity. In a world where capital and labor cannot move between locations, the neoclassical paradigm solves for location-specific first-best policies. Counterfactuals in these models are then the distributional and global welfare gains from imposing Pigouvian taxes relative to a laissez-faire baseline.

Economic geography models: The alternative leading approach uses tools from the economic geography literature, namely dynamic spatial general equilibrium models. The economic geography framework allows for high spatial resolution and offers modeled agents a more broad choice set in exchange for abstracting from some aspects of intertemporal choice. Desmet and Rossi-Hansberg (2015) is the first of these models – a two sector IAM with costless mobility of labor and abstract borders – that examines the heterogenous effects of climate change on migration, trade, and welfare. State-of-the-art models building on this work such as Nath (2020), Conte et al. (2021), Rudik et al. (2021), Burzyński et al. (2022), Cruz (2023), and Cruz and Rossi-Hansberg (2023) incorporate more realistic geographies as well as local variation in fundamental amenities, productivities, and the frictions associated with the movement of goods and agents.³ A drawback to this approach is that the functional forms for utility and investment are restrictive: bilateral migration is always feasible between any two locations as migration costs cannot bind, mobility decisions often collapse to static (rather than forward-looking) choices, and modeled workers typically live hand-to-mouth (i.e., are unable to shift consumption intertemporally). Agents’ only mechanism in these

³The economic geography models exhibit an exceptional degree of richness. Features include endogenous natality, trade, and migration on the agents’ side along with new technology adoption and increasing marginal extraction costs faced by firms in the emitting sectors.

models for insuring their future consumption is to move to a location with higher productivity levels.

This paper is intended to serve as a first step in bridging the gap between the two workhorse model paradigms, an avenue suggested in the recent research agenda posited by Desmet and Rossi-Hansberg (2024) for the literature on multi-region models of climate change. The closest work in the dynamic spatial general equilibrium literature considering climate change is Bilal and Rossi-Hansberg (2023) in which they form a county-level model of the United States that examines how climate change affects local capital accumulation while allowing workers to move between locations. In their model, the anticipated effects of climate change can shape current capital accumulation (and in turn, current wages and migration decisions). However, as capital is owned solely by local entrepreneurs, workers (the agents who migrate) remain hand-to-mouth agents who make decisions solely over mobility. While capital dynamics affect the expectations of future wages for forward-looking agents through both actual and anticipated changes in capital accumulation, workers themselves are unable to alter their consumption/savings patterns as a channel of adaptation to climate change.

My paper also has similar aspects to that of Barbosa Alves and Braulio (2023), who form a partial-equilibrium model of outmigration from rural areas in Guatemala to the United States in response to climate shocks. Like my paper, theirs combines real migration costs and incomplete markets and shows that the value of migration as insurance against climate shocks is sensitive to household income levels. This paper abstracts from incorporating feedback between economic activity and climate change that would close my model as a traditional IAM. Unlike Krusell and Smith (2022) and Cruz and Rossi-Hansberg (2023), I assume a fixed pathway for global temperatures based on benchmark forecasts in the literature and abstract entirely from the endogenous effects of economic activity on climate change. I also abstract from agglomeration and crowding externalities present in other spatial models which are key determinants of location choice within countries (Desmet, Nagy, and Rossi-Hansberg 2018) and would help discipline some of the results I present here. Work incorporating the richness of spatial models that both preserves the intertemporal substitution channel for adaptation and endogenizes the aggregate externality of climate change remains the gold standard and natural avenue for future research.

2 A Two-Period Warming World

In this section I present a two-period version of my full model. The model highlights the importance of both savings and mobility in a world where climate change shifts the

distribution of local productivity levels over time. In the first period, agents receive their endowments and decide whether to migrate as well as how much to lend and borrow on the capital market. In the second period, the effects of climate change are realized. Agents receive factor income based on their savings and the prevailing local wages in each location. When returns to capital are exogenous, extreme cases of the model nest analogues of neoclassical and economic geography models. Intuitive comparative statics follow directly: emigration shares are increasing in local warming and declining in migration costs. Critically, when migration requires an up-front cost paid with real consumption goods, constraints on borrowing can prevent modeled agents from moving to areas less-affected by climate change. This result is contextualized in the simple setting and motivates the inclusion of both channels for adaptation in the fully calibrated model.

2.1 Model Environment

The world consists of a continuum of islands indexed by i on the interval $[0, 1]$. It lasts for two periods, indexed 1 and 2. Climate change is realized in period 2, which causes each island to experience damages to local productivity levels. The islands are populated by a unit mass of *ex-ante* identical agents distributed uniformly in the first period. Each atomistic agent has identical utility over consumption on each day and is endowed with a single unit of labor which they supply inelastically. Let the function $L_t(i)$ denote the density of agents on island i at a given point in time.

Agents face two decisions in the first period: whether to move to a different island, and how much of their first period income to save. In order to move from location i to j , agents must forego $m(i, j)$ units of first-day consumption. I assume this cost is non-negative, continuously differentiable when $i \neq j$, and zero for agents that do not move ($m(i, i) = 0, \forall i$). The cost may be asymmetric such that $m(i, j)$ is not necessarily equal to $m(j, i)$. The limiting case, $m(i, j) = \infty, \forall i \neq j$ where no agents move, represents the most stylized version of the neoclassical model. Agents on all islands additionally have access to a global capital market which allows them to borrow or lend at the risk free rate r . Assume initially this market consists of a large enough number of borrowers and lenders such that the agents' collective savings decisions do not affect the interest rate. Saving an amount S of the consumption good in the first period allows them to receive additional income of $(1 + r)S$ in the second period. When borrowing is prohibited, the model resembles an economic geography framework.

Agents' income on the first day is a uniform endowment $y(i) = y$ across all islands. On the first day, an agent on island i faces a budget constraint over savings S , first-period consumption c_1 , and the costs of migration m :

$$y = S(i, j) + m(i, j) + c_1$$

where arguments (i, j) denote the agent's savings and migration costs conditional on starting in island i and choosing to move to island j .

In the second period, after agents have moved, each island experiences an idiosyncratic degree of damages from climate change. For simplicity, I assume the economic effects take the form of a shock to labor-augmenting productivity in the second period $A_2(i)$ that is given by a multiplicative exponential function:

$$A_2(i) = \exp\left(\frac{-\theta(i)}{1-\alpha}\right)$$

where climate damages $\theta(i)$ parameterize the extent to which climate change affects output in each location.⁴ Agents have full information over both the initial distribution of the population as well as the level of flooding that will occur on each island prior to production on the second day leaving no aggregate uncertainty.

Production in the second period is facilitated by a representative firm on each island. All firms have access to identical Cobb-Douglas technology that uses capital K and effective labor AN to produce the consumption good:

$$Y_2(i) = K_2(i)^\alpha (A_2(i)N_2(i))^{1-\alpha}$$

Each representative firm may rent an unrestricted level of capital on the global market at rate r . Labor markets operate in autarky; the firm on each island may only hire labor from residents who reside there. As labor is supplied inelastically, in equilibrium demand for labor on each island is equal to the number of agents residing there. Equilibrium wages on each island on the second day are

$$w_2(i) = A_2(i)(1-\alpha)\left(\frac{\alpha}{r}\right)^{\frac{\alpha}{1-\alpha}}$$

Finally, I assume each atomistic agent in a given location i draws an idiosyncratic set of additive taste shocks associated with each one of her potential next-period locations,

⁴Note these effects can, in principle, be positive or negative. I implicitly assume all $\theta(i)$ are elements of the set $\{\bar{\mathbb{R}} \setminus -\infty\}$ such that wages are finite for all locations in the second period.

$\{\lambda(j)\}_{j \in [0,1]}$, prior to migration decisions. The shocks are independent draws from a Type-1 extreme value distribution with variance $\pi^2/6$ and scale parameter one, lending a convenient closed form for the resulting policy functions.⁵ Let $W(i, j)$ denote the conditional value function (defined as the return net of taste shocks) of moving for an agent who begins on island i and moves to island j :

$$\begin{aligned} W(i, j) = \max_{S(i,j)} & \left\{ (1 - \beta) \ln(c_1(i)) + \beta \ln(c_2(j)) \right\} \\ \text{s.t.} & \quad c_1(i) = y - S(i, j) - m(i, j) \\ & \quad c_2(j) = w_2(j) + (1 + r)S(i, j) \end{aligned} \tag{1}$$

the expression in (1) is the maximized value of utility from consumption across both periods for an agent who begins at location i and migrates to location j net of her idiosyncratic taste shocks. Each agent who starts in location i can express her two-period problem, the choice over her second-period location j , as a function of her taste shock draws and the conditional desirability of islands:

$$V(i) = \max_j \left\{ \lambda(j) + W(i, j) \right\} \tag{2}$$

The probability an agent at location i chooses location j as her second period destination induced by the problem in (2) is given by a closed form function of exponentiated conditional values across all destinations. The probability of choosing destination j given origin i is:⁶

$$\pi(i, j) = \frac{e^{W(i,j)}}{\int_0^1 e^{W(i,k)} dk} \tag{3}$$

Definition: A spatial competitive equilibrium given damages $\{\theta(i) : i \in [0, 1]\}$ consists of savings policies $S(i, j)$, migration shares $\pi(i, j)$, prices $w_2(j)$ and r , and second-period allocations for each representative firm $(N_2(j), K_2(j))$ such that:

1. Taking prices as given, savings policies $S(i, j)$ and migration levels $\pi(i, j)$ maximize consumers' conditional problem for all location pairs (i, j)

⁵Although this assumption is non-essential, it is ubiquitous in the discrete choice literature (Train 2009) and substantially aids tractability (Iskhakov et al. 2017) when taken to the calibrated model.

⁶Both the density of agents moving from location i to j as well as the share of agents in location i making this decision are equal to $\pi(i, j)$ as the initial distribution is uniform over the measure one set of islands.

2. Given prices and damages, firms' second-period decisions over hiring and capital rental ($N_2(j), K_2(j)$) are optimal in all locations

3. Migration levels $\pi(i, j)$ lead to second-period populations that clear labor markets

$$\int_0^1 \pi(i, j) di = N_2(j), \forall j$$

2.2 Properties of Equilibrium

When r is set exogenously, wages in all locations are determined by local productivity levels and the global interest rate. This ensures a unique equilibrium, as the distribution of agents in the second period is solely a function of exogenous factor prices and migration costs. Although it is substantially more parsimonious, the two-period model mirrors several outcomes in the neoclassical and economic geography frameworks.

Lemma 1. *It is optimal for agents to populate all locations regardless of damages in the second period.*

Proof. As $m(i, i) = 0$ by assumption, $W(i, i) \geq k > -\infty$ for all islands as long as the gross interest rate is positive (i.e., $1+r > 0$). It follows from the fact that $W(i, j)$ is bounded for all (i, j) pairs that $\pi(i, i)$ is strictly positive for all i . \square

The lemma shows that regardless of how extreme the local effects of climate change will be on a given island, there are always agents who will stay even if losses reduce second period labor income to zero. This feature is not an artifact of functional forms; Lemma 1 would hold for an arbitrary distribution of second-period productivities and migration costs or if production technology were linear. In equilibrium, we may also observe agents move to islands with lower ex-ante conditional values than their original location despite perfect foresight. Imposing agents forego consumption goods to migrate helps discipline this aspect of the model:

Lemma 2. *For a given location i , if migration costs are sufficiently large no agents move.*

Proof. Any $m(i, j) > y + (1+r)^{-1}w_2(j)$ ensures no agents move from i to j as doing so would lead to negative consumption. If this cost is sufficiently large for all destinations $j \neq i$, no agents move. \square

To illustrate the implications of Lemma 2 consider the case of migration costs from island i being fixed at $m(i, j) = \tilde{m}$ for all potential destinations $j \neq i$. Figure 1 shows how increasing this cost lowers the share of agents $\pi(i, -i)$ who leave the island in equilibrium. When the cost of emigration \tilde{m} rises past $\bar{y} = y + (1+r)^{-1}w_2(j)$, where $w_2(j)$ is the highest equilibrium second-period wage, no agents who begin on island i are able to emigrate regardless of how second-period wages there may be. Similar forces, namely the relative sizes of income and migration costs, cause liquidity constraints to restrain migration in the full model. This feature also helps the model replicate the large number of zeros in bilateral migration flows between countries observed in the data (Grogger and Hanson 2011) and low emigration rates from poor areas generally despite large wage differences (Lagakos, Mobarak, and Waugh 2023).^{7,8}

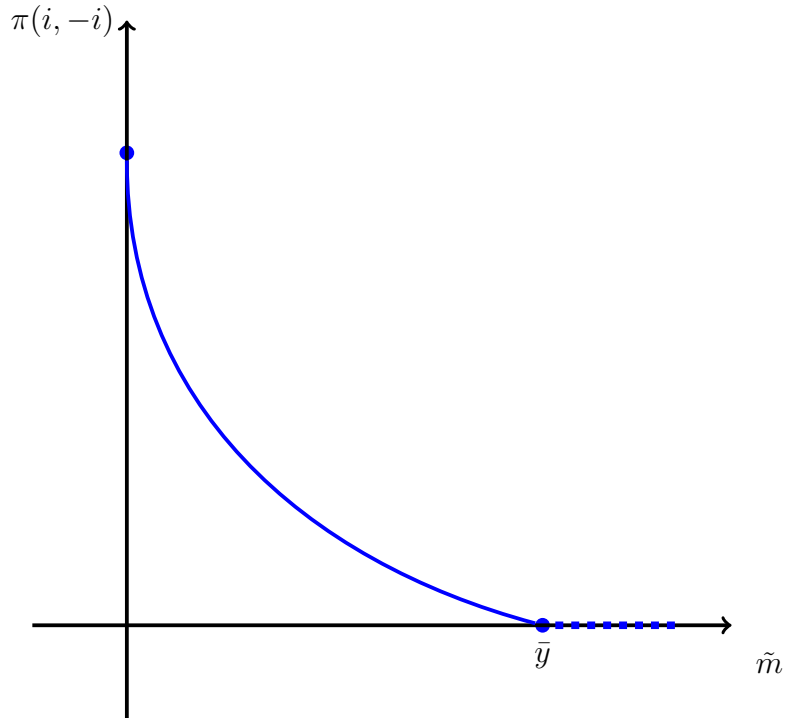


Figure 1: Share of Leavers as a Function of Migration Costs

⁷This is consistent with the finding that emigration poses a substantial financial cost (as opposed to a loss of utility alone) in many countries (Clemens, Montenegro, and Pritchett 2019). This result can be refined by precluding borrowing, which will in general further reduce emigration from poor areas even when wage gaps are large. Other frameworks that model migration costs as utility losses (c.f. Cruz and Rossi-Hansberg 2023) typically do not condition these shocks on income and cannot capture this income-dependent constraint. Modeling savings causes the ability to emigrate to be jointly determined by both wealth and migration costs.

⁸Zeros comprise over 25 percent of the estimated bilateral migration flow values between the 154 countries I use in the full model. This figure rises to over 50 percent of all flows under more conservative demographic accounting methods (Abel and Cohen 2022).

Incorporating moving costs seems critical for determining the effects of climate change on migration patterns. Evidence from field and natural experiments also suggests that high migration costs in tandem with liquidity constraints play a substantial role in explaining why agents remain in low-productivity areas despite existing wage gaps (Bazzi 2017; Cai 2020).⁹ Lemma 2 shows how the model allows for these features to shape equilibrium outcomes and can allow different propensities to migrate for poor and rich agents in the same location.

Finally, comparative statics on how changing migration costs and damages affect the share of agents who migrate are tractable and intuitive:

Proposition 1. *Holding r constant, an increase in the cost of migration raises the share of stayers $\pi(i, i)$ in all locations. An increase in damages $\theta(i)$ lowers the share of arrivals it receives, $\pi(j, i)$, from all islands.*

Proof. See Appendix A. □

When the demand for savings plays no role in determining the equilibrium interest rate, the effect of increasing migration costs is unambiguous. Raising costs lowers the net benefit of moving to a higher-wage location. The share of agents staying on each island between periods one and two increases on all islands, and is offset by a decline in emigration to other islands. An intuitive converse holds for the local effects of larger second-period damages. Low idiosyncratic productivity on that island lowers wages while having no effects on wages in all other locations due to the interest rate being fixed. Both these static results also attain in the limiting economic geography case where savings is prohibited.

Proposition 2. *An increase in r raises the share of stayers in all locations with above-average productivity in the second period. The effect is ambiguous for places with below-average productivity.*

Proof. See Appendix B. □

The effects of varying r are less clear; increasing r raises the share of agents who stay on the more-fortunate islands. The gains from increased returns on savings not spent on migration become larger relative to any gains from taste shocks or even higher wages. However, this does not necessarily hold true for agents on the worst-hit islands. The local wage losses from higher interest rates may be large enough to increase emigration even as borrowing costs rise.

⁹The presence of liquidity constraints fails to explain the dearth of migration in some settings. Lagakos, Mobarak, and Waugh (2023) argue for seasonal migration in Bangladesh that low rates of uptake by poor households are due to it being an expensive form of insurance.

2.3 Endogenous r

Fixing r exogenously lends the simple model clean insights. However, as climate change (and the exercise of this paper) is global, it is possible to refine the equilibrium concept to ensure that the supply of capital meets demand:

4. The capital market clears at rate r

$$\int_0^1 K_2^D(j) dj = \int_0^1 \int_0^1 \pi(i, j) S(i, j) di dj \quad (4)$$

where

$$K_2^D(j) = A_2(j) N_2(j) \left(\frac{\alpha}{r} \right)^{\frac{\alpha}{1-\alpha}}$$

This additional condition closes the simple model in general equilibrium. Appendix C proves at least one equilibrium exists when (4) holds. While the preliminary Lemmas hold in this setting, imposing general equilibrium breaks the clean results presented in Proposition 1. The effect of changing migration costs or $A_2(i)$ in isolation on the share of stayers is ambiguous.¹⁰ As suggested by Proposition 2, this occurs because any knock-on effects on equilibrium interest rates can have ambiguous effects on the rate of stayers in low-wage locations due to the opposing forces of lower wages and higher borrowing costs. Shifts in equilibrium interest rates caused by increased migration costs may have different effects for agents who borrow in order to move (for whom it costs more to migrate) versus those who gain more from staying in place. This indeterminacy holds even for the case where multiple equilibria are ruled out.¹¹

The simple model highlights the importance of both space and time as distinct channels for adaptation to changing climate. The model suggests at some point we should expect agents to use real resources to avoid areas worst hit by climate change. However, solely allowing for adaptation through location choice misses the ability for agents to partially insure by substituting intertemporally.¹² Determining outcomes when both channels are available requires modeling the intersection of these two channels for adaptation.

¹⁰See Appendix D for a proof.

¹¹Appendix E shows that even in the case where the equilibrium is unique, the effects of changes in migration costs or second-period productivities on the share of stayers cannot be signed without strong assumptions on the joint distribution of migration costs and productivity shocks.

¹²Firms' decisions in Cruz and Rossi-Hansberg (2023), the preeminent SIAM, do allow for a form of investment in the sense that firms' choose a level of technological innovation each period, but their problem reduces to a static one and this investment does not allow agents to smooth consumption through savings by selling claims on the firms' profits. Other spatial formulations allow for capital accumulation, but the agents that do so cannot migrate (c.f. Bilal and Rossi-Hansberg 2023).

3 A Model of Global Savings and Migration

The rest of the paper takes the framework of the two-period model to a calibrated infinite-horizon setting. The world is separated into regions which operate in autarky. A large number of agents are distributed among the regions, each of which has a representative firm with access to production technology with location-specific productivity. Firms must hire local labor, but have access to an integrated world capital market that rents out agents' savings at a uniform risk free rate. Each period, agents choose a (potentially new) location as well as how much wealth to carry into the next period. Outside of preference shocks determining location choices, agents face idiosyncratic risk over their ability to supply labor. This section outlines the model structure and defines an equilibrium concept for the model in a steady-state. As the only risks are idiosyncratic, the steady-state environment is in the tradition of Aiyagari (1994). While individual agents' locations and wealth levels change over time, the aggregate distribution of agent types by location is stationary before climate change begins shifting the distribution of productivity levels across locations.

3.1 Agents

The world is populated by a continuum of infinitely-lived agents of measure one, each identical in their preferences and discount factors who live in one of N locations each period. Time is discrete. Agents supply labor inelastically to a representative firm in their location which produces a single uniform good that can be consumed or saved in the form of capital. Like in Aiyagari (1994), agents face idiosyncratic risk to their labor supply. Labor endowments s fluctuate between a high h and low ℓ state that follows a Markov process with transition probabilities $P(s'|s)$ denoted by $\Pi_{ss'}$, such that an agent in location i receives labor income sw_i that period.

As in the two-period model, each agent receives a set of location-specific idiosyncratic i.i.d. taste shocks each period denoted by $\{\lambda_t(i)\}_{i=1}^N$. Agents must pay a fixed amount of the consumption good to migrate between regions. Agents pay an amount of the consumption good $m(i, j)$ each period to migrate between locations i and j . The cost function here is assumed to be non-negative, allowed to be bilaterally asymmetric, and satisfies $m(i, i) = 0$. This modeling choice acknowledges that migrants cannot overcome the barriers between borders through pure disutility alone. The mechanism here instead reflects the fact that international migration net of physical travel costs, whether it is visa fees or golden passports, is never entirely free of charge (Recchi et al. 2021; Surak 2021).

Agents choose savings a each period, which they lend out to a frictionless global capital market. Firms in each region can rent capital at a risk-free rate r_t net of depreciation. I

assume agents' borrowing is constrained by a lower bound of \underline{a}_t each period, which may be greater than or equal to the natural borrowing limit. The set of possible assets holdings \mathcal{A} is the interval $[\underline{a}_t, \infty)$. Each agent's problem is to form a plan for sequences of conditional savings decisions and location choices $\{a_\tau, j_{\tau+1}\}_{\tau=0}^\infty$ that maximizes her expected lifetime utility:

$$\begin{aligned} V_t(a_t, s_t, j_t, \{\lambda_t(i)\}_{i=1}^N) &= \max \mathbb{E}_t \sum_{\tau=0}^{\infty} \beta^{t+\tau} (\ln(c_{t+\tau}) + \lambda_{t+\tau}(j_{t+\tau+1})) \\ \text{s.t.} \quad &s_{t+\tau} w_{j,t+\tau} + (1 + r_{t+\tau}) a_{t+\tau} = a_{t+\tau+1} + c_{t+\tau} + m(j_{t+\tau}, j_{t+\tau+1}) \\ &a_{t+\tau+1} \geq \underline{a}_{t+\tau} \quad , \quad \forall \tau \\ &a_t, s_t, j_t, \{\lambda_t(i)\}_{i=1}^N \quad \text{given} \end{aligned} \quad (5)$$

subject to her budget constraint, her current idiosyncratic shocks, and the sequence of period-specific borrowing limits $\underline{a}_{t+\tau}$.

3.2 Production

The measure of agents residing in location j with labor supply s holding assets a at time t is denoted by $\Omega_t(a, s, j)$. The total level of agents in each location j at time t can be expressed as

$$L_{j,t} = \sum_{a \in \mathcal{A}} \sum_{s \in \ell, h} \Omega_t(a, s, j) \quad (6)$$

Production is operated by a representative firm in each location. All firms have access to an identical Cobb-Douglas production technology which combines capital K and effective labor as inputs to produce a uniform final good. Each period, labor supplied by all agents in location j is

$$N_{j,t}^S = \sum_{a \in \mathcal{A}} \sum_{s \in \ell, h} \Omega_t(a, s, j) s$$

Each location is endowed with a fundamental level of labor-augmenting productivity \bar{A}_j reflecting the large variation in per-capita incomes observed in the data. I assume migration costs and productivity grow at a rate of g each year such that productivity in all locations can be expressed as $A_{j,t} = \bar{A}_j(1 + g)^t$. Firms take both the (global) rental rate for capital r_t and local wages $w_{j,t}$ as given and employ labor and capital up to the point where profits are

zero. Equilibrium wages may then be written solely as a function of the global interest rate r_t and local fundamental productivity levels:

$$w_{j,t} = A_{j,t}(1 - \alpha) \left(\frac{\alpha}{r_t + \delta} \right)^{\frac{1}{1-\alpha}}$$

Which implies that equilibrium capital demand in each location satisfies

$$K_{j,t}^D = A_{j,t} N_{j,t}^D \left(\frac{\alpha}{r_t + \delta} \right)^{\frac{1}{1-\alpha}}$$

3.3 Recursive Formulation

At this point it is convenient to transform the agent's problem in (5) into a stationary form before expressing it recursively. When productivity growth is constant, the path of endogenous variables can be expressed in normalized terms such that they do not grow without bounds. Define $\gamma = (1 + g)$ such that $A_{j,t} = \gamma^t \bar{A}_j$. Let hat values

$$\hat{z}_t \equiv \frac{z_t}{\gamma^t}$$

denote the value of all endogenous variables normalized by cumulative productivity growth at period t relative to the initial period. The agent's sequential problem can be rewritten as

$$\begin{aligned} V_t(a_t, s_t, j_t, \{\lambda_t(i)\}_{i=1}^N) &= \max \mathbb{E}_t \sum_{\tau=0}^{\infty} \beta^\tau (\tau \ln(\gamma) + \ln(\hat{c}_{t+\tau}) + \lambda_{t+\tau}(j_{t+\tau+1})) \\ \text{s.t.} \quad &\gamma^\tau s_{t+\tau} \hat{w}_{j,t+\tau} + (1 + r_{t+\tau}) \gamma^\tau \hat{a}_{t+\tau} = \gamma^{\tau+1} \hat{a}_{t+\tau+1} + \gamma^\tau \hat{c}_{t+\tau} + \gamma^\tau \hat{m}(j_{t+\tau}, j_{t+\tau+1}) \\ &\hat{a}_{t+\tau+1} \geq \hat{a} \\ &\hat{a}_t, s_t, j_t, \{\lambda_t(i)\}_{i=1}^N \quad \text{given} \end{aligned} \tag{7}$$

Rewrite the function on the left hand side of Equation (7) in stationary form

$$\gamma^t \hat{V}_t(\hat{a}_t, s_t, j_t, \{\lambda_t(i)\}_{i=1}^N) = V_t(a_t, s_t, j_t, \{\lambda_t(i)\}_{i=1}^N)$$

and divide through by γ^τ in the budget constraint. This normalized value function solves the functional equation:

$$\hat{V}_t(\hat{a}_t, s_t, i_t, \{\lambda_t(j)\}_{i=1}^N) = \max_j \left\{ \max_{\hat{a}_{t+1} \in \Gamma(\hat{a}_t, s_t, i_t)} \left\{ u(\hat{c}_t) + \lambda_t(j) + \beta \mathbb{E}[\hat{V}_{t+1}(\hat{a}_{t+1}, s_{t+1}, j_{t+1}, \{\lambda_{t+1}(k)\}_{k=1}^N)] \right\} \right\} \quad (8)$$

$$\text{s.t. } (1+r_t)\hat{a}_t + \hat{w}_{i,t}s_t = \gamma\hat{a}_{t+1} + \hat{c}_t + \hat{m}(i, j), \\ \hat{a}_{t+1} \geq \underline{a}_t$$

for all location pairs (i, j) where \hat{a}_{t+1} is her savings in effective units conditional on a choice of next-period location j and $\Gamma(\hat{a}_t, s_t, i_t)$ is the constraint correspondence governing her possible actions given her current state.¹³ The policy functions that maximize the right-hand side of equation (8) coincide with the sequence of (normalized) decisions that maximize (7).

Let $\hat{x}_t := \{\hat{a}_t, s_t, i_t\}$ summarize an agents' state variables (her current asset holdings, labor endowment, and location). Let $\hat{d}_t := \{j, \hat{a}_{t+1}\} \in \Gamma(\hat{x}_t)$ be the tuple of her choice variables over location and asset holdings next period, where $\Gamma(\hat{x}_t)$ is the constraint correspondence rewritten as a function of her state \hat{x}_t . Finally, let $u_t(\hat{x}_t, \hat{d}_t)$ be her returns in state \hat{x}_t when she chooses decision \hat{d}_t . When the taste shocks over locations, $\{\lambda(k)\}$, are independent draws from a Type-1 extreme value distribution with scale parameter one for all agents, Rust (1987) shows the conditional expectation of her value function $\mathbb{E}[\hat{V}_{t+1}|\hat{x}_t, \hat{d}_t]$, rewritten as $\mathbb{E}[V_{t+1}(\hat{x}_t, \hat{d}_t)]$, is the solution to the contraction mapping $T(\mathbb{E}[V_{t+1}(\cdot)]) = \mathbb{E}[V_{t+1}(\cdot)]$ for each (\hat{x}_t, \hat{d}_t) tuple defined by¹⁴

$$\mathbb{E}[\hat{V}_{t+1}(\hat{x}_t, \hat{d}_t)] = \sum_{s' \in \ell, h} \Pi_{ss'} \ln \left(\sum_{k_{t+1}} \exp \left(\max_{\hat{a}_{t+2} \in \Gamma(x_{t+1})} \left\{ u_{t+1}(\hat{x}_{t+1}, \hat{d}_{t+1}) + \beta \mathbb{E}[\hat{V}_{t+2}(\hat{x}_{t+1}, \hat{d}_{t+1})] \right\} \right) \right) \quad (9)$$

The right hand side of equation (9) is the expected continuation value for an agent in state \hat{x}_t who makes decision \hat{d}_t for her next-period location and asset holdings. It averages the expected value of being in the state \hat{x}_{t+1} that results from choice \hat{d}_t today across each of the potential choices she may make in period $t+1$, conditional on how the Markov process Π will determine her labor supply in the future. The value from each potential choice \hat{d}_{t+1} tomorrow is then determined by her (correct) expectation that, she will choose a savings level

¹³In a slight abuse of notation I've also swapped the notation such that the (i, j) convention is preserved for describing origins and destinations.

\hat{a}_{t+2} that maximizes the argument of the exponential term for each of the possible locations in period $t + 2$ she may choose.

Define her savings policy conditional on choice of location, $g_t(\hat{x}_t, k_t) := \hat{a}_{t+1}$, which solves the interior maximization problem in (9) for each choice of location and corresponds to the optimal decisions in the sequential problem. The functional form of the shocks also leads to a closed-form solution for the probability an agent in state \hat{x}_t will find it optimal to move to location j in period $t + 1$. By a law of large numbers argument, this probability is also the share of agents of type \hat{x} who move to location j , and is given by¹⁴

$$\pi_t(\hat{x}, j) = \frac{\exp\left(u_t(\hat{x}_t, \hat{d}_t^j) + \beta \mathbb{E}\left[\hat{V}_{t+1}(\hat{x}_t, \hat{d}_t^j)\right]\right)}{\sum_{k=1}^N \exp\left(u_t(\hat{x}_t, \hat{d}_t^k) + \beta \mathbb{E}\left[\hat{V}_{t+1}(\hat{x}_t, \hat{d}_t^k)\right]\right)} \quad (10)$$

where the notation $\hat{d}_t^j := \{j, g_t(x_t, j)\}$ denotes the vector pairing her location decision with the associated optimal savings level. These probabilities along with a joint distribution of wealth and labor endowments across locations determines the evolution of the distribution of agents. Given a distribution of agents $\hat{\Omega}_t(\hat{a}, s, i) \equiv \hat{\Omega}_t(\hat{x})$ across locations, the distribution of agents of type $\hat{x}' = (\hat{a}', s', j')$ at time $t + 1$ is given by

$$\hat{\Omega}_{t+1}(\hat{x}') = \sum_{\hat{x}} \hat{\Omega}_t(\hat{x}_t) \Pi_{ss'} \mathbb{I}[g(\hat{x}_t, j') = \hat{a}'] \pi(\hat{x}_t, j') \quad (11)$$

I now turn to defining a stationary equilibrium for this economy, where $\hat{\Omega}(\hat{x})$ in (11) along with the normalized value functions and conditional choice probabilities in Equations (9) and (10) are time-invariant.

3.4 Equilibrium

Definition: A Stationary Recursive Competitive Spatial Equilibrium (SRCE) equilibrium consists of a set of expected value functions $\mathbb{E}[\hat{V}(\hat{x}, \hat{d})]$, savings policies $g(\hat{x}, j)$, migration probabilities $\pi(\hat{x}, j)$, an interest rate r and effective wages at each location $\{\hat{w}_i\}_{i=1}^N$, and a joint distribution of wealth and labor endowments across locations $\hat{\Omega}(\hat{x})$ such that:

- Given prices $(r, \{\hat{w}_i\}_{i=1}^N)$, savings policies $g(x, j')$ and $\mathbb{E}[\hat{V}(\hat{x}, \hat{d})]$ solve functional equation (9) and induce the probabilities in (10)

¹⁴Technical issues arise when applying a conventional law of large numbers argument to economies characterized by a continuum of agents who experience idiosyncratic shocks governed by realizations of random variables. Uhlig (1996) provides a weaker criterion for convergence in probability such that the large numbers argument invoked here, that migration probabilities induce an equal share of agents to move, holds formally.

2. Given prices $(r, \{\hat{w}\}_{i=1}^N)$, firms' factor demand \hat{K}_h^D and N_h^D are optimal in all locations
3. The global capital market clears at interest rate r

$$\sum_{h=1}^N \hat{K}_h^D = \sum_{\hat{x}} \hat{\Omega}(\hat{x}) \sum_{j=1}^N g(\hat{x}, j) \pi(\hat{x}, j)$$

4. Labor markets clear at effective wage \hat{w}_h in each location h

$$N_h^D = \sum_{\hat{a}} \sum_s \hat{\Omega}(\hat{a}, s, h) s, \forall h$$

5. The joint distribution of agents over asset holdings, labor endowments, and locations $\hat{\Omega}(\hat{x})$ is stationary in that it is a fixed point of the transition function induced by migration probabilities $\pi(\hat{x}, j)$ and policy functions $g(\hat{x}, j)$

In a stationary equilibrium, the economy behaves as a model of discrete choice over locations where each location choice nests a standard consumption/savings problem with uninsurable risk. When the economy is parameterized with only one region it nests a version of Aiyagari (1994) with productivity growth and two states of possible labor supply. Appendix F provides an overview of the solution algorithm for solving the optimal policy and value functions as well as for the SCRE. I briefly discuss the numerical issues with this type of dynamic model where agents face both discrete and continuous choices (Iskhakov et al. 2017) as well as how multiple equilibria issues in Aiyagari economies (Walsh and Young 2024) may be exacerbated in my setting where aggregate effective labor supply is also determined by the equilibrium distribution of agents.

3.5 Discussion

I adopt an incomplete markets model as idiosyncratic income shocks have been shown to be key determinants of individuals' decisions over international migration (Gröger and Zylberberg 2016; Bazzi 2017). As the process governing shocks is independent of location and wealth levels, it is intended to capture a broad notion of uninsurable income risks agents face around the world that may interact with decisions to migrate. In low-income regions where a large share of workers are employed in agriculture, these shocks can be interpreted as local weather fluctuations, which have been shown to drive migration and labor reallocation (Colmer 2021; Barbosa Alves and Bráulio 2023). However, these shocks may also comprise

those affecting employment more broadly, as declines in local labor demand can lead to internal migration in settings beyond the agricultural sector (Cai 2020).

More generally, when the costs of migration enter agents' budget constraints, migration rates in a given region can vary across the local income distribution. As illustrated by Lemma 2 in the simple model, this is because the set of agents who face binding constraints on migration is determined by both wealth and local wages. This reflects that international emigration is increasing in income at low income levels both within countries and in the cross sectional data (Cai et al. 2016; Bazzi 2017) because of factors such as credit constraints and large up-front costs (Clemens, Montenegro, and Pritchett 2019; Lagakos, Mobarak, and Waugh 2023). Both of these frictions can become barriers to migration in the model; the agents in a given origin region for whom migration costs are prohibitively high is an endogenous outcome in equilibrium.

4 Calibration of the Baseline Economy

This section takes a version of the model with $N = 154$ regions, each corresponding to a country, to the data. The model is calibrated such that the equilibrium shares of the global population in each country predicted by the model match observed average shares for the five-year period between 2010 and 2014. Solving for the baseline equilibrium requires inputs for the structural parameters governing the model, namely the fundamental productivity and initial temperature levels in each country, pairwise bilateral migration costs between each country, and the deep parameters governing production and preferences. Sections 4.1 and 4.2 list the parameters which I set directly based on external sources – those either taken from the literature or set directly based on the observable analogues. Section 4.3 turns to listing the remaining parameters in the model that I estimate using the method of simulated moments described in Section 4.4.

4.1 Parameters Sourced from Existing Estimates:

Fundamental Productivities and Population Levels: Fundamental baseline productivity levels are assigned based on the 2010-14 average of real per capita GDP as-recorded in the World Bank's World Development Index (WDI – WBG 2016). I normalize this measure of labor-augmenting productivity such that all values are relative to that of the United States in 2010. The target moments for the baseline economy are based on each country's average share of the global level over the same five-year period in the WDI.

Projections of Future Climate Change: I form projections for temperature trajecto-

ries between 2015 and 2100 using output from the Coupled Model Intercomparison Project Phase 6 (CMIP6). The Coupled Model Intercomparison Project provides a consensus on a set of standardized experiments that allow for climate modelers to coordinate the design and comparison of output on a harmonized basis (Eyring et al. 2016). I focus on two benchmark scenarios for anthropogenic greenhouse gas emissions, Representative Concentration Pathways (RCPs) 4.5 and 8.5, which are indexed numerically according to the associated increases in radiative forcing by 2100 (Van Vuuren et al. 2011).¹⁵ The RCPs are a set of paired socioeconomic and greenhouse gas emissions trajectories between 2005 and 2100 (Van Vuuren et al. 2011), each guided by a qualitative narrative for how the world develops as a whole over the coming century (Lee et al. 2021). Higher indices indicate larger increases in forcing and with it cumulative warming. To form RCP-specific projections of future temperatures out through 2100, I use the simple average of annual warming across outputs from 33 modeling groups participating in the CMIP6. The projections provide annual averages of near-surface temperatures at the $1^\circ \times 1^\circ$ resolution globally for each of the two RCPs I consider. I then aggregate the grid scale temperature data into population-weighted average annual temperatures in each country using gridded population data (base year 2015) from the Gridded Population of the World version 4 (GPWv4 – CIESIN 2017) and boundaries from the Global Administrative Database (GADM 2022).

Historical Temperatures: I use a process analogous to that for future temperatures to construct population-weighted average temperatures at the country level. Baseline temperatures in each country, \bar{T}_j , are constructed as arithmetic averages of population-weighted temperatures between 1955 and 2014, where time-invariant weights are again assigned using the GPWv4 data (CIESIN 2017).

Climate Damages: Nath, Ramey, and Klenow (2023) use local projection methods along with country-level panel data on temperature and GDP to estimate country-specific response functions for how climate change affects output growth.¹⁶ These projections combine to form estimates of the cumulative effects of temperature increases on output growth, $D_j(\bar{T}_j, \Delta T_{j,t})$, for each country in the panel they use for estimation. I use these cumulative response functions to fit a parameterized function $D(\bar{T}_j, \Delta T_{j,t})$ that maps country-level historical averages temperatures, \bar{T}_j , and future changes in local temperatures due to climate change, $\Delta T_{j,t}$, into contemporary effects on productivity growth. For country j that experiences an increase average annual temperatures of $\Delta T_{j,t}$ in year, t , the resulting effects on productivity growth are given by

¹⁵I am grateful to Jamie Scott at the University of Colorado for facilitating an easy file transfer process for accessing the data containing these ensemble averages.

¹⁶I thank Ishan Nath for providing the point estimates from Nath, Ramey, and Klenow (2023).

$$\frac{\Delta A_{j,t}}{A_{j,t}} = g + \frac{D(\bar{T}_j, \Delta T_{j,t})}{1 - \alpha} \quad (12)$$

where the $1 - \alpha$ term in the denominator of the second term ensures the damages to labor-augmenting productivity in my model translate to the estimated losses in output growth found in NRK.

4.2 Directly Chosen Parameters

Labor Supply Shocks: I normalize the high labor productivity level s_h to one, and set the low productivity state s_ℓ to 0.2. This level is halfway between zero (a complete loss of labor income) and the level of 0.4 which is a common parameterized value for unemployment benefits (Shimer 2005). I set $\Pi_{\ell h}$ and $\Pi_{h\ell}$, the transition probabilities into (out of) the high state, to match an equilibrium share of about 9 percent of agents in the low state

$$\begin{bmatrix} \Pi_{hh} & \Pi_{\ell h} \\ \Pi_{h\ell} & \Pi_{\ell\ell} \end{bmatrix} \begin{bmatrix} h \\ \ell \end{bmatrix} = \begin{bmatrix} h \\ \ell \end{bmatrix} = \begin{bmatrix} 0.91 \\ 0.09 \end{bmatrix}$$

and an expected bad shock duration of two years.

$$\mathbb{E}[\text{Time in Low State}] = (1 - \Pi_{\ell\ell}) \sum_{t=1}^{\infty} t \Pi_{\ell\ell}^{t-1} = 2$$

Asset Grid: In the main experiment, I set the lower bound on normalized asset holdings to 0 which precludes borrowing entirely. Two factors drive this decision. First, because per-capita wages are exceptionally low in many countries relative to global averages, the natural borrowing limit is already very low for many agents. Without adding an additional vector that would track state-contingent borrowing limits for each agent, the global borrowing limit (which must be weakly greater than the minimum of all state-continent natural borrowing limits) becomes essentially zero. Second, in models of low-income settings it is common to assume commitment is asymmetric and prevent agents from borrowing even when they have access to risk-free savings (Lagakos, Mobarak, and Waugh 2023).

Deep Parameters: All other parameters that are chosen externally are shown in Table 1, which displays the values as well as their source in the literature. These parameters govern pure time preference, the capital share in production, depreciation, productivity growth, and agents' coefficient of relative risk aversion.

Table 1: Externally Calibrated Parameters

Parameter	Value	Source
α	0.3	Golosov et al. (2014)
β	0.985	Golosov et al. (2014)
δ	0.06	Krusell and Smith (2022)
g	0.01	Piketty (2014)
Coefficient of Relative Risk Aversion	1	Acemoglu (2008)
s_h	1	Normalized
s_ℓ	0.2	Shimer (2005)
a	0	Lagakos, Mobarak, and Waugh (2023)

4.3 Parameters to Estimate

I estimate the remaining parameters governing the model. This includes the matrix of pairwise migration costs between all countries – the set of $m(i, j)$ terms – along with three additional structural error parameters δ_C , δ_I , and δ_H that aid model fit.

Structural Error Terms: The structural error terms allow for the modeled results to be reconciled with two facts in the data: (1), that a vast majority of agents do not migrate in a given year; and (2), that despite relatively low wages, a large portion of the worlds' population lives in China and India. To account for these facts, I add three additive utility shifters to the model (the structural error terms) which give additional utility each period to agents living in China, agents living in India, and agents who choose not to migrate, denoted δ_C , δ_I and δ_H respectively. Thus an agent who expects to live in China (India) in period t receives unconditional utility of $u(c_t) + \delta_C$ (δ_I) and an agent who chooses not to move receives additional utility of $u(c_t) + \delta_H$.

Migration Matrix: The set of pairwise bilateral migration costs is the only remaining model input unavailable in the data. While estimates of the implicit monetary barriers to international migration exist for some origin-destination pairs (e.g., Clemens, Montenegro, and Pritchett 2019), there is nowhere near a consensus dataset containing even a small portion of these values. Instead, I allow the entries in this matrix to be free parameters to be estimated such the stationary equilibrium of the model absent climate change matches the shares of the global population living in each modeled country we see today.

Estimating each of the $N(N - 1) = 23,562$ bilateral migration costs as separate free parameters would be both computationally intractable and would require calibrating the

model directly on observed bilateral migration moments from the data. To reduce the number of free parameters, I adopt a functional form for migration costs that is based on the income quartile of the two countries along with the Euclidean distance between their population-weighted coordinate centroids. Migration costs to go from country i to country j consist of three components:

$$m(i, j) = m^o(q_i) + m^d(q_j) + \bar{m}_1 \rho(i, j) + \bar{m}_2 \rho(i, j)^2, \forall i \neq j \quad (13)$$

where in a slight abuse of notation, the values $m(i, j)$ in equation (13) from here forward denote the time-invariant values in equation (7) that are normalized relative to productivity growth each period.

The origin and destination fixed effects, $m^o(q_i)$ and $m^d(q_j)$, are determined by the income quartiles q_i and q_j of the origin and destination country. Each possible origin country is assigned a fixed emigration cost across all possible destinations, $m^o(q_i)$, based on the income quartile of that country in the 2010-14 period. The same procedure assigns a cost to immigrate to each country, $m^d(q_j)$, based on its income quartile. The third and fourth terms are an additive cost that is a function of distance between the origin and destination countries parameterized by a quadratic function in the Euclidian norm between the countries' population-weighted centroids $\rho(i, j)$. This allows migration costs to reflect the fact that holding income levels constant, bilateral population flows decrease in distance travelled in the data (Abel and Cohen 2022). This substantially reduces the number of free parameters (from over 20,000 to 13) while allowing for heterogeneity in bilateral migration costs at the country level and for asymmetric bilateral moving costs between all country pairs.

4.4 Estimation

I estimate the free parameters in the model (see Section 4.3) which govern migration costs and structural error terms using the Method of Simulated Moments (MSM). This approach searches for the set of 13 parameter estimates $\hat{\Theta} = \{\{\hat{m}^o(q)\}_{q=1}^4, \{\hat{m}^d(q)\}_{q=1}^4, \{\hat{m}_i\}_{i=1}^2, \hat{\delta}_C, \hat{\delta}_I, \hat{\delta}_H\}$ which minimizes the distance between the share of modeled agents living in each country in predicted in equilibrium and the observed shares of the global population residing in each country between 2010 and 2014. The estimates are parameter values which minimize the gap between observed shares of global population in each country – \tilde{L}_j – and the equilibrium population shares in the model – $\bar{L}_j(\theta)$ from equation (6) – when it is parameterized by a given candidate vector θ . Modeled shares $\bar{L}_j(\theta)$ are calculated for each candidate θ using the stationary distribution it induces, $\Omega^\theta(a, s, j)$, and evaluating the share of the population

residing in each country in equilibrium:¹⁷

$$\bar{L}_j(\theta) = \sum_a \sum_s \Omega^\theta(a, s, j) \quad (14)$$

The targeted moments are the distance between the modeled population shares in equilibrium, $\bar{L}_j(\theta)$, in each country and the global population in each country \tilde{L}_j we observe in the data

$$z_j(\tilde{L}_j, \theta) = (\tilde{L}_j - \bar{L}_j(\theta)) \quad (15)$$

When the model is correctly specified, the MSM identifies the parameters governing the population shares we see in the world, \tilde{L}_j . This relies on the assumption that the moment functions in (15) satisfy

$$\mathbb{E}[z_j(\tilde{L}_j, \Theta)] = 0 \quad (16)$$

for some unique vector of parameters Θ which governs the true data generating process. The MSM takes the 154 moment conditions from each country across each country and minimizes their generalized norm by solving:

$$\hat{\Theta} = \underset{\theta}{\operatorname{argmin}} \mathbf{z}(\tilde{L}, \theta)' W \mathbf{z}(\tilde{L}, \theta) \quad (17)$$

where $\mathbf{z}(\tilde{L}, \theta)$ is a vector of each moment condition from equation (15) and W is the identity matrix. Estimate $\hat{\Theta}$ is the set of migration cost parameters and structural effects that calibrate the model to the period ranging from 2010 to 2014.

5 Estimation Results

Figure 2 gives a visual display of the calibration errors when evaluated at the estimated values of $\hat{\Theta}$ produced by the MSM. These values measure how well the model replicates observed shares of the global population who resided in each country during the 2010-14 period. For each country, the map displays the value of $z_j(\tilde{L}_j, \hat{\Theta})$ measured in the percentage point (p.p.) difference between model and observed population shares. Countries with a darker red (blue) shade are those where the model under- (over-) predicts the steady-state share of the global population who inhabits that country relative to the data. The R^2 is 0.78; the

¹⁷I solve for the labor supply in each region under an exogenous interest rate $r = 0.9\beta^{-1}(1+g)$ only once for each candidate θ . I do not solve the full SCRE (inclusive of the interest rate at which the capital markets clear) for each migration matrix candidate as doing this is too computationally intensive at this time.

model accounts for about three-quarters of observed variation.

Even with the aid from the three structural error terms and heterogenous bilateral migration costs, the model struggles to rationalize the share of low- (high-) productivity countries that have large (small) populations. The largest errors (in magnitude) are in China and India, where despite the addition of structural error terms δ_C, δ_I the model undershoots steady-state population shares by three and four points respectively. Similar issues emerge for Indonesia, for which (especially without an additional structural term) the model struggles to match its large population relative to its productivity level. Conversely, the model over-predicts steady-state populations in most of Northern Europe. This is driven by forces complementary to those which motivate the structural error terms, namely that these countries have simultaneously (very) high productivity levels and small populations. Modeled population shares in the Netherlands, Austria, Switzerland, Denmark, Norway, and Sweden all exceed their data analogues by between two and three percentage points due to their exceptionally high productivity levels and low distance from neighboring countries in Europe. This latter feature (namely the over-prediction of initial population shares in Europe) proves quantitatively important when evaluating aggregate welfare changes from climate change in the sections below due to assigning too much weight to the modeled agents in Europe who gain from warming.

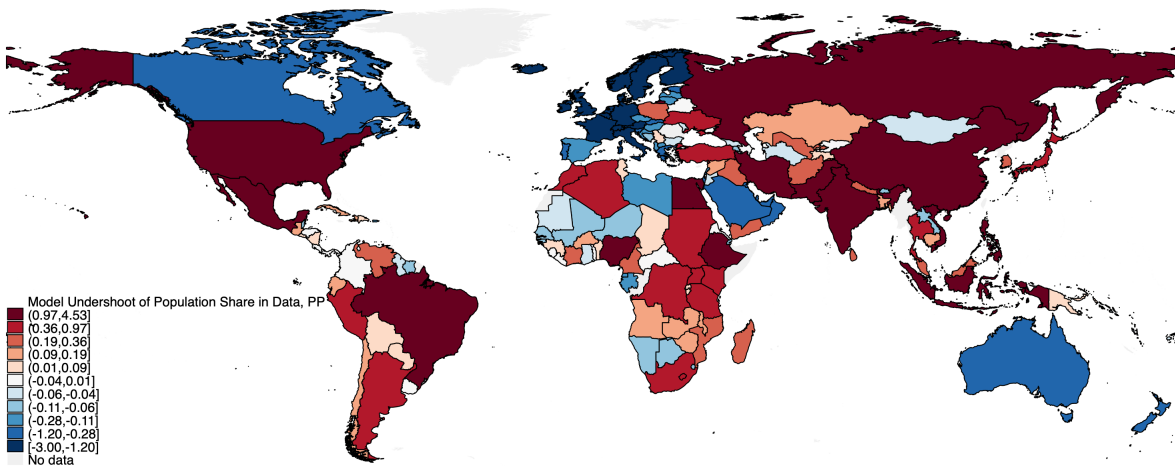


Figure 2: Baseline Model Calibration Errors, (p.p.)

Table 2 displays a few specific bilateral migration cost pairs generated by the estimated parameter values $\hat{\Theta}$ which govern the steady-state population levels and migration shares in the calibrated model. To give a sense of scale, rather than reporting the raw values from the model, each cost $\tilde{m}(i, j)$ in Table 2 is reported as the ratio of estimated $m(i, j)$ values relative to \hat{w}_{USA} – equilibrium normalized wages in the United States. Migration between

geographically close countries of similar income levels tends to be the least expensive form; fitted values imply it costs about 16% of annual U.S. wages to go between Benin and Togo (neighboring small countries in Western Africa) or to migrate between Norway and Sweden (neighboring medium countries in Northern Europe). This translates to about \$6,900 in 2019 dollars when taken to the real output values in the WDI data (WBG 2016).

Costs to go between countries separated by larger distances or income gaps tend to be higher. The estimated cost of travel from Guatemala to the United States is 19% of U.S. wages (roughly \$8,200), while the extreme case of going from Bangladesh to Switzerland has estimated costs of 28% of U.S. wages (\$12,000). While it is not a direct comparisons in terms of the objects identified by the model, the magnitudes of costs to emigrate from poor to rich countries match implied barriers to migration estimated in the literature using empirical methods. Clemens, Montenegro, and Pritchett (2019) estimate barriers to low-skilled migration for a panel of 42 low-income countries relative to the United States and find implied costs of between \$5,000 and \$24,000 annually. Bazzi (2017) reports that migration costs from Indonesia to Southeast Asia and the Middle East through temporary work programs costed \$1,250 in 2019 dollars.¹⁸

Table 2: Example migration costs as share of modeled U.S. wages

Origin-Destination Pair	$\tilde{m}(i, j)$
Benin → Togo	0.160
Norway → Sweden	0.164
Guatamala → USA	0.187
Bangladesh → Switzerland	0.284

The calibrated model, as well as others in the spatial economics literature, imply high financial barriers to movement that prohibit poor agents from migrating.

Figure 3 shows the analogue of Figure 1 in the stylized model. Each line shows the share of agents who emigrate from a given location in the calibrated model generated by the migration policy functions:

$$\Pr(\text{Stay in country } i | \hat{x}) = 1 - \sum_{j \neq i}^N \pi(\hat{x}, j)$$

¹⁸I inflate these levels from the values in Bazzi (2017) using the PCE implicit price deflator for the United States so as to have a rough comparison between values in real levels.

across varying levels of wealth \hat{a} for four different origin countries. Like in the stylized case, as agent's wealth (not including wages) nears zero, the probability agents stay in place becomes one in most countries. This proves critical for determining emigration in countries where income is low; the blue and green lines in Figure 3 show respectively these probabilities for two low-income countries in very different geographies, Togo and Haiti. Well-over half of the agents who reside in each of these countries in the steady state of the calibrated model cannot migrate due to the inability to borrow enough to pay for the up-front cost. Their only avenue for adaptation is then to either increase savings locally so as to smooth income in place or eventually meet the costs of moving.

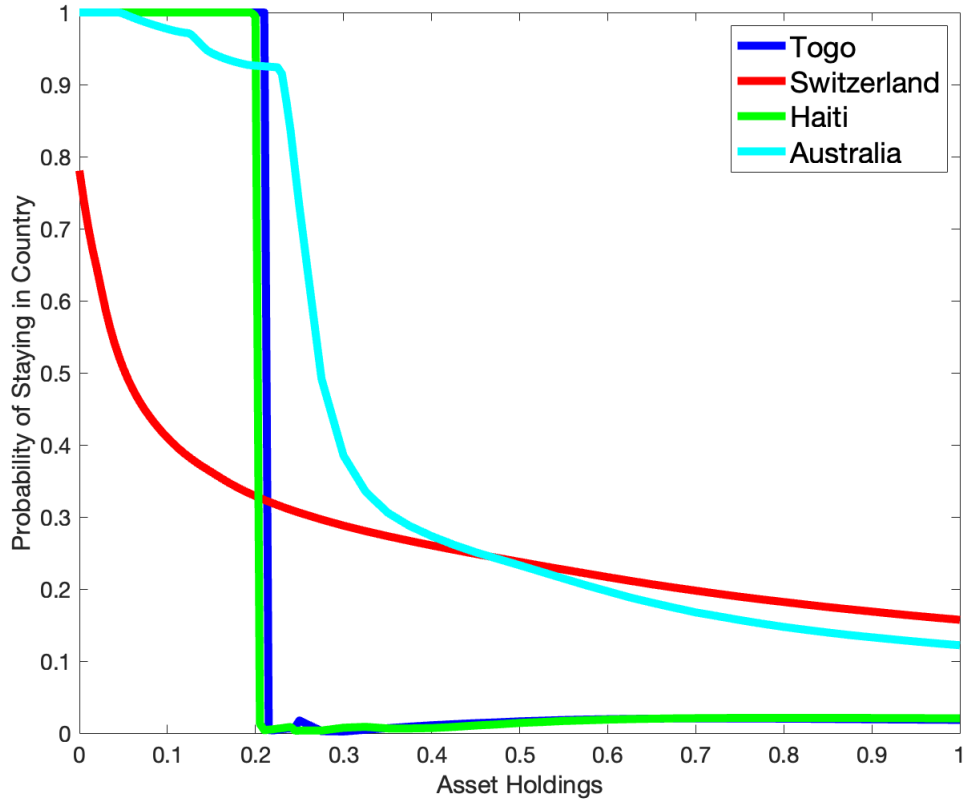


Figure 3: Migration Probabilities as a Function of Wealth in Poor and Rich Countries with Low and High Migration Costs

A converse result is generated for wealthy countries regardless of moving costs. The model substantially over-predicts the propensity for agents in high-income locations to move, as shown by the probabilities of staying in place for Australia and Switzerland (cyan and red lines in Figure 3). While higher migration costs for Australians due to the large distance

between its population-weighted centroid and neighboring countries do lead to some constraints on migration not felt by modeled Swiss, the probability of staying in place falls to about 10 percent for agents in both countries when these probabilities are evaluated at the median wealth level there. However, while the model almost certainly displays too much movement among wealthy agents according to their taste shocks, this is not the case for poor (constrained) agents. When the model is used to forecast population dynamics while the world warms, this ensures that for the agents for whom borrowing constraints and up front costs are large barriers to using international migration as adaptation, I do not over-predict their response.

6 Case Study: Colombia and Venezuela

Lemma 2 illustrated in a simplified setting how the response of migration to climate change will depend crucially on how high migration costs are relative to real income levels. Calibrating these costs directly from observed migration patterns is difficult as there are limited historical cases where large waves of international migration have been both driven by shocks to productivity and well-documented by national statistical agencies. This renders calibrating the model based on observed climate-driven shocks infeasible and motivates my limitation of targeted moments to the current distribution of population globally rather than historical population flows.¹⁹ The goal of this section is to show that under a reasonable parameterization of the model, it can qualitatively replicate the dynamics of historical episodes of productivity-driven emigration.

Outside of the effects of violent conflict and the dissolution of the Soviet Union, the largest recent historical population change at the national level is the case of Venezuela in the 21st century. In March of 2013, the then-leader of Venezuela Hugo Chavez passed away. The country subsequently experienced a period of hyperinflation that coincided with an unprecedented collapse in output and productivity. Between 2013 and 2019, measured productivity in Venezuela fell by 90 percent. This collapse in productivity lead to a huge outflow of people from Venezuela to Colombia as well as other neighboring countries, as shown in Appendix Figures G.1 and G.2. While this is a distinct shock from those likely to be induced by future climate change, it is the only recent event where macroeconomically significant migration flows may be reasonably attributed to declines in productivity.²⁰

¹⁹This is not to say there have not been large bouts of historical emigration in response to extreme weather events which may have been made more likely by climate change. The Horn of Africa is currently experiencing a protracted drought that has displaced millions of people; unfortunately these effects are not yet readily visible in harmonized global population series ([see here](#)).

²⁰Evidence that historical climate change increased the likelihood of civil conflict (Hsiang, Meng, and

I run a validation exercise to test whether the general framework in this model is able to replicate observed population dynamics across Colombia and Venezuela after 2013. Given bilateral migration costs that allow me to exactly fit the two observed population levels in Colombia and Venezuela in the pre- and post-Chavez periods, how well does the model match the observed transition dynamics and how large must migration costs be relative to modeled wages?²¹ The transition period I consider is the years 2014-2019 in the data for the population shares and productivity levels in Venezuela and Colombia. Modeled agents learn (with certainty) the full extent of collapse that occurs starting in 2014 and react accordingly until the model reaches a new steady state.²² Appendix Figure G.3 displays time series for the shares of combined population in Colombia and Venezuela in data between 2014-19 as well their modeled counterparts. Solid lines show the dynamics produced by the model transition path while the dashed lines are values taken from the data (labeled “data” in the figure). “Time since Shock” measures the number of years elapsed since 2014. The model slightly overshoots the pace of net emigration from Venezuela in response to the initial shocks; modeled Venezuelan population share always lies below observed levels in Figure G.3 after 2014. However, on the whole the model is able to qualitatively match the resulting emigration dynamics seen in post-collapse Venezuela with only two free parameters.

7 Projections under Climate Change

The calibrated model serves as a laboratory to examine how the effects of climate change on productivity will shape global population dynamics during the 21st century. This section uses both steady-state comparisons and transition path exercises to examine these effects at various time horizons. I first use the steady-state comparison framework to perform three experiments exhibiting the relative importance of damages and migration costs in determining the *long-run* effects on the global population distribution. Each experiment solves for a new steady-state of the global economy after the world has adjusted to warming through 2100 induced by a given emissions trajectory. The first, which I refer to as the baseline forecast, examines the change in the steady-state of the global economy caused by the roughly 2.0 °C of warming under RCP4.5. The second re-examines what the steady state would look like in 2100 under the warming induced by RCP8.5 (approximately 4.2 °C). Finally, I examine the extent to which the new steady state changes if in addition to

Cane 2011) lends an additional degree of credence to this connection if future productivity declines can be in-part attributed to this specific mechanism.

²¹Figure G.1 in the Appendix presents sufficient statistics for calibrating a pre-2014 stationary equilibrium, a transition path of productivity levels in Venezuela, and a post-shock steady state in 2019.

²²A full description of how I take the model to these data can be found in Appendix G.

the productivity effects of warming under RCP4.5 are realized, migration costs are doubled globally.

The transition path portion of the analysis focuses instead on the short- and medium-run effects of climate change in the modeled economy. This generates a forecast for global population dynamics for the entire 21st century as the world warms and adjusts towards a new steady state. In the transition analysis, each agent in the economy learns in the first year of the transition path that future climate change under RCP4.5 will alter the trajectory of global productivity levels in the next 85 years. Each period, agents make new migration and savings decisions according to their new expectations for how climate change will affect future wages and interest rates given that these changes will become more pronounced as warming intensifies. Because of the slow onset of warming, the experiment differs somewhat from traditional transition paths between stationary equilibria in the macroeconomics literature (c.f. Conesa and Krueger 1999) as agents act according to the expected future changes induced by climate change before much of the damages are realized. This exercise (unlike the steady-state comparisons) allows for explicit calculation of how long the world takes to adjust to the new steady state as well as the individual-level welfare effects of climate change across the full distribution of modeled agents.

7.1 The Long-Run Effects of Warming

The first counterfactual experiment focuses on how both the short and long-run global distribution of where people will live be affected by climate change in the 21st century. I assume the new long-run climate under each RCP is determined by the cumulative level of warming predicted by the ensemble average across projections from the Coupled Model Intercomparison Project Phase 6 (CMIP6) for 2100 (Eyring et al. 2016). I focus on RCP4.5, a “middle-of-the-road” scenario for emissions which induces a relatively modest increase in forcing relative to that of RCP8.5, which is generally recognized as a pessimistic path for future global emissions. I use it a baseline here not as a “business-as-usual” scenario for emissions – RCP8.5 currently tracks most-closely with emissions to date among the five central scenarios used by the IPCC (Schwalm, Glendon, and Duffy 2020) – but rather one that reflects some degree of mitigation at the global scale implemented in the next century. However, analogous results for the effects of RCP8.5 as opposed to the baseline scenario for local warming and productivity growth are given in parenthetical values throughout this section where applicable.

Warming: Figure 4 displays a map of projections from CMIP6 ensemble average for mean anthropogenic climate change (ACC) that will occur by 2100 across the globe under

RCP4.5 (RCP8.5).²³ Each country is colored according to the difference in annual average temperatures between the calibrated 2010-14 period and the mean forecast across the CMIP6 model outputs for 2100. Warming is increasing in latitude, with countries in Europe and North America projected to warm the most while southern portions of Africa and South America experience less pronounced temperature changes. The world warms by a projected 2.0 °C (4.2 °C) on a population-weighted basis.

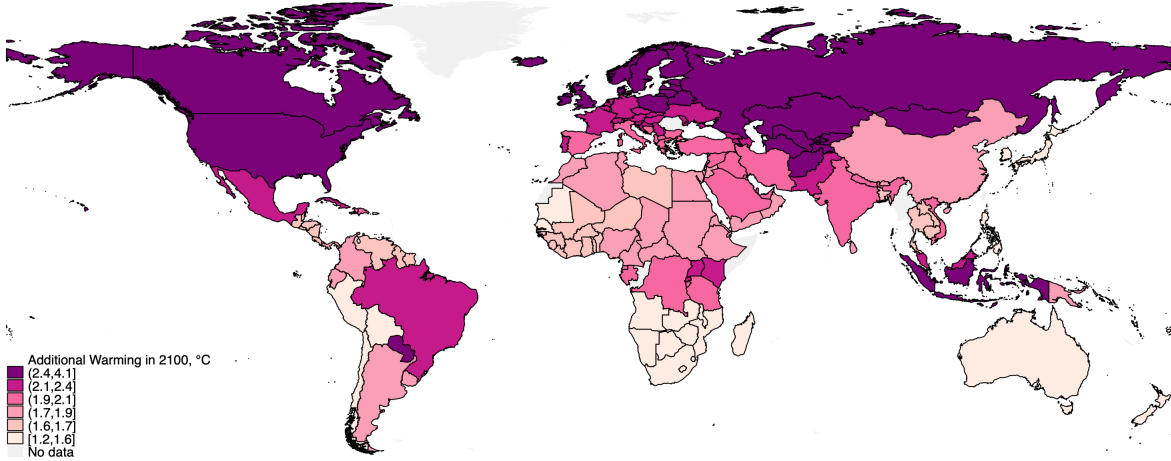


Figure 4: Forecast Warming in 2100 (°C) Under RCP4.5

Damages: Figure 5 maps the warming in Figure 4 into changes in cumulative productivity growth by 2100 using damage values based on estimates from Nath, Ramey, and Klenow (2023). Each country is colored according to how climate change will affect cumulative productivity growth relative to baseline using the mapping in Equation (12) that simplifies the damage functions in NRK. Countries in the deepest shade of blue experience the largest drags on productivity growth, while those in dark green experience the largest gains from warming. As productivity loss from climate change follow today’s temperature gradient, both the sign and magnitude of the changes in productivity growth induced by warming vary quite a bit globally. Current warm places are forecast to experience the largest losses, while cold climates today experience large gains. The unweighted mean (median) change in country-level cumulative productivity growth through 2100 is a loss of 5.5 (10.9) percentage points (p.p.). This decline is substantial – it marks a decline in cumulative growth larger than five (ten) years of modeled baseline growth over that period. The lost productivity growth is highly diffuse geographically – the standard deviation in losses is 13 percentage

²³The level of warming in Figure 4 is roughly 1 °C less than warming from pre-industrial levels under either RCP as it is measured relative to a 2015 baseline.

points. While warm countries like Indonesia experience losses of 20 p.p. of growth, the coldest countries today, such as Iceland and Mongolia, experience gains of over 50 additional percentage points relative due to the effects of climate change.

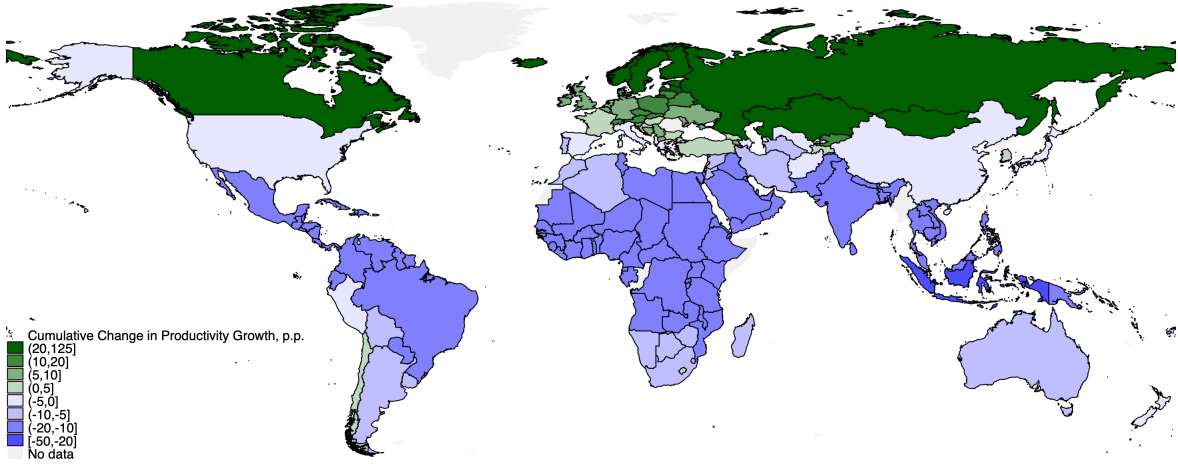


Figure 5: Cumulative Change in Productivity Growth by 2100 (p.p.) Induced by Climate Change

Population Shares: Figure 6 shows how the global population distribution changes in the new steady-state relative to the modeled version of today. Countries in darker shades of blue (green) experience larger declines (increases) in their shares of global population (measured in percentage points) under the new climate when compared to the baseline distribution calibrated to 2010-14. Unlike in other spatial models (c.f. Cruz and Rossi-Hansberg 2023), while there is net migration Northward (towards regions that gain from climate change), the gradient of population changes is not monotonically increasing in latitude.

Six percent of the world population relocate (on net) to different countries after the cumulative effects of warming through 2100 are fully realized. The largest population declines in terms of percentages of initial (steady-state) population levels occur in the United States, Australia, Japan, and Western Europe. This result is not because these locations are worst hit, but instead because the agents in these locations have sufficient income such that more of them prefer to move to locations in Northern Europe or Canada which are forecast to experience productivity gains. A non-negligible amount of emigration occurs in places which are relatively cold initially, as these baseline cold places tend to be near even colder which experience even larger gains from climate change. The model predicts an especially large decline in the population of the United States (almost 50% of baseline levels) as emigration to Canada is an easy way to trade forecast local damages for the gains north of the border.

Unlike other spatial models of climate change, despite the large degree of migration that occurs between rich countries in response to climate change, the amount of emigration from the worst-hit poor countries is limited. Forecast changes in populations in Sub-Saharan Africa, a region where both baseline productivities are relatively low and the impacts of climate change are forecast to be very negative are all lower than 0.1 percent of the global population. This is because, as discussed in Section 5, a large fraction of agents who reside in poor countries are unable to borrow or save up to the point of having enough wealth to move. Their only avenue for adaptation is then to either increase savings locally so as to smooth income in place or eventually meet the costs of moving.

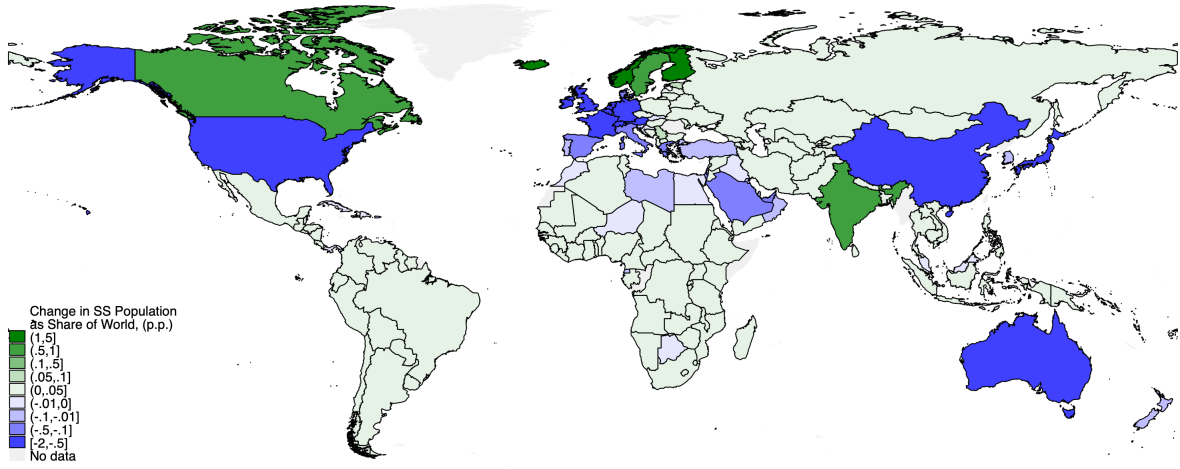


Figure 6: Change in Country-Level Shares of Global Population in New Steady-State, RCP4.5

7.2 Transition Analysis under RCP4.5

For the transition analysis, I initialize the model in its pre-climate change steady state and feed in a trajectory of warming between 2015 and 2100 based on the projections from the modeling groups participating in the CMIP6. After the shock is realized, agents have correct expectations over the trajectory of warming (and in turn, all other endogenous aggregate variables) over the entire transition period. The full algorithm for the numerical calculation of the economic dynamics under climate change is described in Appendix H, but is qualitatively similar to the standard approach outlined in Conesa and Krueger (1999).

Population Dynamics: A first output of the transition analysis is the full path of how the global population in the model responds to climate change in each year as the emissions pathways under RCP4.5 begins in 2015. Figure 7 shows how both the population distribution

(grey circles) and global temperatures (dashed blue line) change each year relative to the calibrated steady state starting in 2015 out through the new steady-state after 2100 (shown as a cross section in Figure 6). The blue line shows the population weighted change in annual average temperatures under RCP4.5 based on projections from the CMIP6 project; for years after 2100, I assume temperatures settle to the level reached that year. The grey circles show how the share of agents in each country changes relative to the baseline steady state, as measured by sum over all countries of the absolute value of the change in the share of the global population living there. Larger values indicates that (on net) all countries have experienced larger changes in population shares relative to the 2010-14 period.

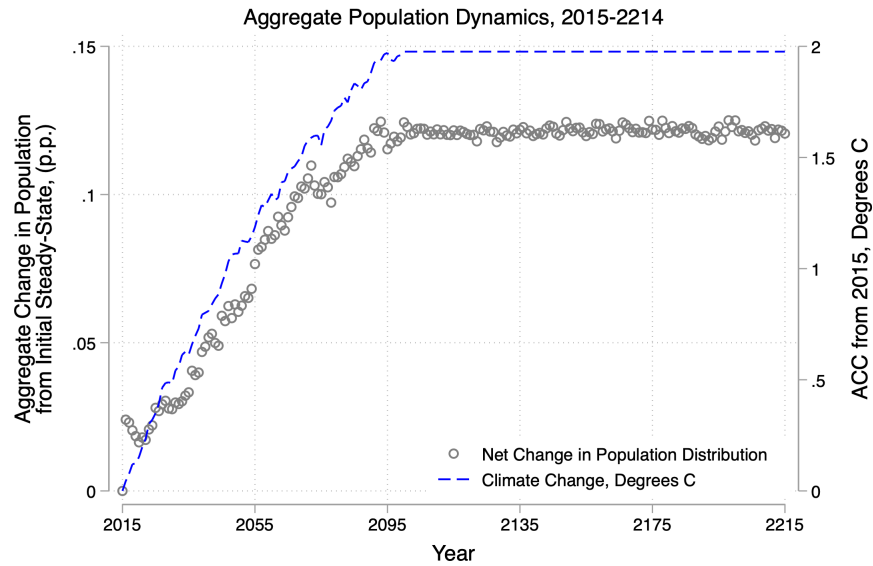


Figure 7: Change in Global Population Distribution vs. Global Average Temperature Change, 2015 - 2215

By 2100, climate change induces a 12 percentage point change in country-level population shares. This corresponds to 6 percent of the global population migrating internationally (on net) in response to climate change. An important aspect of this transition is the speed; the labor side of the model converges to the new steady-state distribution of agents across time very quickly. At the global level, adaptation to climate change through migration precedes realized warming, as shown by the large initial reaction in the years after 2015 when agents realize the shock.²⁴ This large initial shift in agents' location choices highlights prior research on the importance of expectations over future climate change in driving anticipatory

²⁴ Aggregate savings also adjusts fairly quickly, but not the extent to which population changes essentially move in lockstep with warming.

adaptation (Bilal and Rossi-Hansberg 2023).

Welfare: The qualitative advantage of solving for the transition path between steady states is the ability to speak to the changes in welfare induced by climate change. If one simply compares steady states, it's entirely possible that while the transition is costly (requires a substantial amount of moving and savings buildup), welfare is higher on average (or even globally) in the new steady state once the distribution has settled. To have an accurate accounting of the costs incurred by agents during their adaptation to long-run shifts in climate, it's critical to account for the immediate costs that occur along the transition path.

Let $\hat{\Omega}_0$ and $\mathbb{E}[\hat{V}_0(\hat{x}, \hat{g}_0(\hat{x}, j))]$ denote the initial steady state and continuation values in the economy calibrated to the 2010-14 period. For each agent, given their optimal savings decision $\hat{g}_0(\hat{x}, j)$ conditional on location choice j , they (expect to) have a continuation value of $\mathbb{E}[\hat{V}_0(\hat{x}, \hat{g}_0(\hat{x}, j))]$ while the economy remains in steady state. However, along the transition path, climate change alters these continuation values of savings/migration choices to $\mathbb{E}[\hat{V}_{\mathcal{T},1}(\hat{x}, \hat{g}_0(\hat{x}, j))]$ when climate change begins unexpectedly in the first year of the transition period (subscript $\mathcal{T}, 1$). This results in changes in agents' expected welfare in period $\mathcal{T}, 1$ conditional on their decisions prior to the shocks. Summing these effects over all agents

$$\frac{\Delta SW}{SW} = \sum_{\hat{x}} \sum_{j=1}^N \left(\frac{\mathbb{E}[\hat{V}_{\mathcal{T},1}(\hat{x}, \hat{g}_0(\hat{x}, j))]}{\mathbb{E}[\hat{V}_0(\hat{x}, \hat{g}_0(\hat{x}, j))]} - 1 \right) \hat{\Omega}_0(\hat{x}) \pi(\hat{x}, j) \quad (18)$$

gives the change in social welfare due to climate change. The expression equation (18) captures the change in social welfare SW by calculating the aggregate welfare change across all agents in the initial steady-state of the model. Figure 8 shows a histogram of welfare gains and losses across modeled agents.

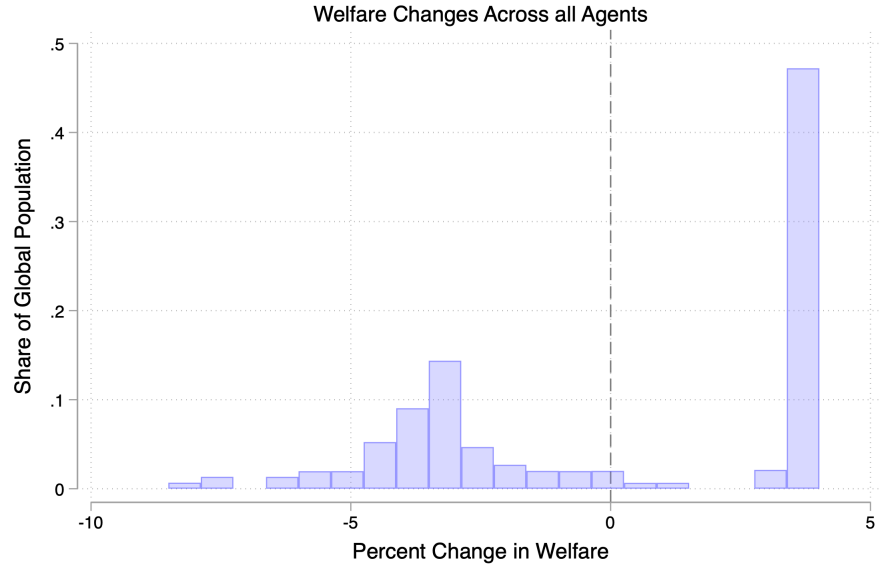


Figure 8: Distribution of Agent-Level Welfare Changes from Climate Change

On aggregate, modeled welfare losses from climate change (the sum of all values in Figure 8) under an RCP4.5 scenario are essentially zero. However, this small aggregate welfare effect masks a highly unequal distribution of gains and losses across rich and poor agents at the individual level. Poor agents in low-income countries such as Indonesia and India face welfare losses of over 8.5 percent, as they are often both the warmest places that are worst-hit by climate change and are unable to afford to migrate. In stark contrast, rich agents who are not constrained can freely migrate towards locations in the global north which are forecast to experience large productivity gains under climate change. Rich agents experience welfare gains of over 4 percent as it is relatively easy for them to reap the projected benefits from warming in already high-productivity locations such as Canada, Northern Europe, and Scandinavia.

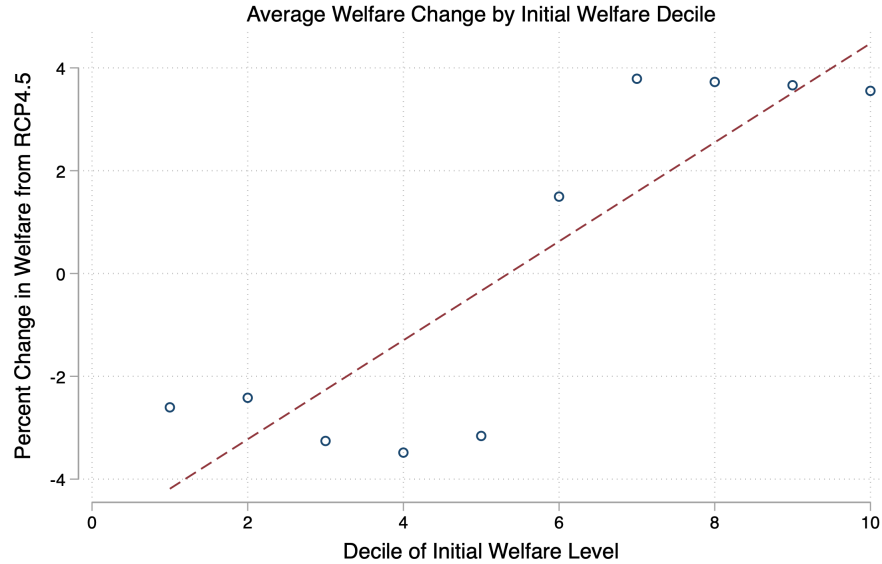


Figure 9: Average Welfare Change by Initial Welfare Level Decile

Figure 9 illustrates which type of agents (in expectation) gain and lose from climate change. The plot shows average welfare gains (losses) by deciles of agents's (expected) welfare from their last decision in steady state prior to entering into the first period of the transition path. The bottom 50 percent of the welfare distribution today experience losses of about 3 percent on average, while the best-off decile today experiences gains from climate change of almost 4 percent on average. Appendix Figure H.1 shows this pattern of inequality also holds if we instead bin agents by their initial wealth holdings (as opposed to initial welfare levels which account for the effects of both financial wealth and location). On the whole, results from the transition path add to the growing body of research that suggests the welfare effects of climate change will be highly unequal both by geography as well as across income groups within a given country.

7.3 Alternative Counterfactuals

I consider two alternative counterfactuals for how future climate change may evolve. I present only the long-run (i.e. steady-state) forecasts here as for these cases it is more informative than the transition paths. The first alternative re-examines what the steady state would look like under a more pessimistic scenario for warming, that induced by the RCP8.5 emissions pathways. The second examines how if in addition to the productivity effects of warming under RCP4.5 are realized, migration costs are concurrently doubled globally.

RCP8.5: Figure 10 displays the analogue of Figure 6 for the changes in steady-state populations after the world warms 4.2°C on average under the RCP8.5 scenario. Appendix Figures I.1 and I.2 show the associated changes in country-level average temperatures and cumulative productivity growth. The extreme productivity changes induced by this pessimistic scenario for emissions cause massive shifts in the global population distribution; 21 percent of the global population migrate internationally when compared to the baseline steady state. However, for the most part the forecast changes under RCP8.5 are exaggerated versions of those in the main model. The lion’s share of migration in Figure 10 takes place as bilateral flows between rich countries and goes Northward towards the Scandinavian countries which experience large additional growth gains (well-over 70 additional percentage points!).

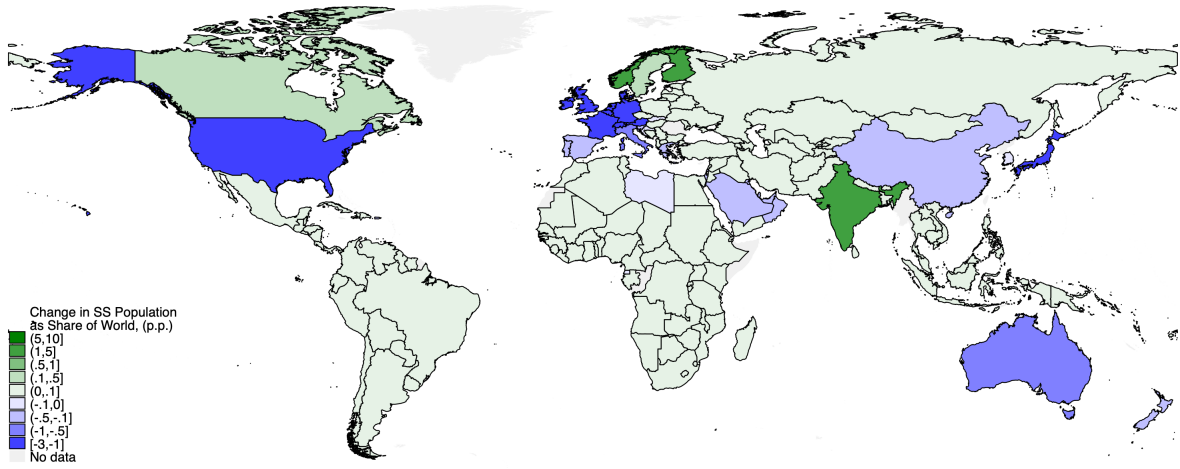


Figure 10: Change in Country-Level Shares of Global Population in New Steady-State, RCP8.5

Doubling of Migration Costs: This scenario considers a world in which, in addition to the warming under RCP4.5, bilateral migration costs $m(i, j)$ are doubled between all country pairs. This reflects the common belief that international migration policies may become less accommodating in the 21st century, especially to any economic migration induced by climate change (Vince 2022). The resulting change in the distribution of the global population is shown in Figure 11. Doubling migration costs makes agents substantially less-sensitive to taste shocks driving migration choices that do not follow the gradient of productivity. As such, almost all modeled agents are either stuck in areas far from Northern Europe where wages are low or end up in Northern Europe and mix only within the Scandinavian countries that receive large productivity gains from warming. The changes in magnitude under this scenario render the forecast somewhat difficult to interpret; I instead view these results as indicative of the extreme importance of considering financial migration costs directly and

taking care to ensure they are calibrated correctly.

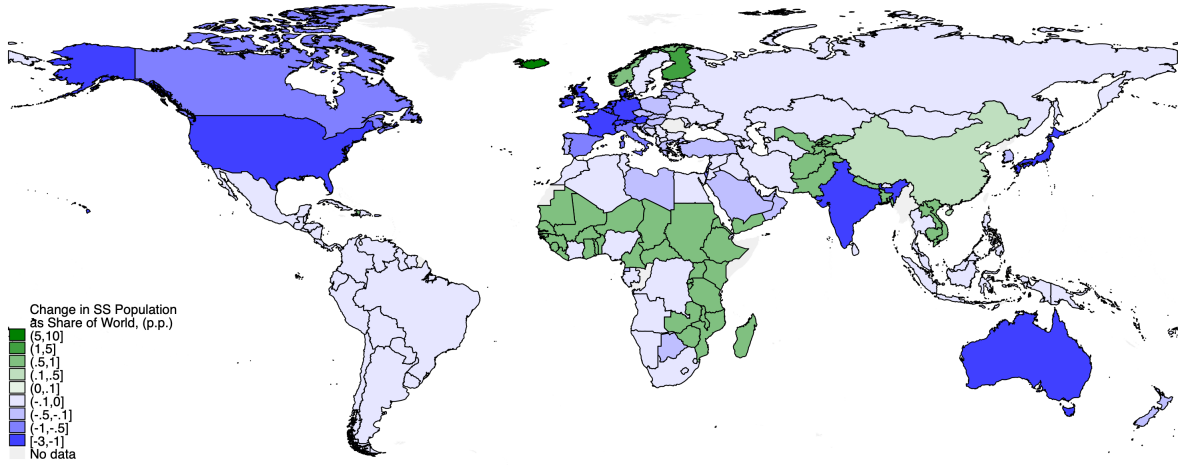


Figure 11: Change in Country-Level Shares of Global Population in New Steady-State, Double Migration Costs

8 Conclusion

This paper presents a global model of population dynamics under climate change in the 21st century. The model nests a neoclassical consumption savings decision within a benchmark dynamic discrete choice spatial framework in order to examine how both local consumption patterns and migration will collectively shape adaptation to climate change. The primary goal of the model is to take seriously the notion that impediments to migration manifest not only through lost utility, but also as explicit up-front financial barriers (Clemens, Montenegro, and Pritchett 2019). Imposing that migrants pay a cost in terms of foregone consumption allows the model to reflect the reality that many people who may otherwise gain from migration from a utility standpoint will be unable to do so due to the frictions they face (Bazzi 2017; Cai 2020).

My main experiment in this paper examines how the global gradient of productivity changes induced by climate change under Representative Concentration Pathway 4.5 shifts the global population both during the 21st century and over a longer-run horizon. The model projects that 6 percent of the global population relocate to different countries when the cumulative effects of warming through 2100 are realized. Despite common narratives suggesting that emigration will be concentrated in the global south (Vince 2022), migration is instead most-concentrated among rich countries and is used as adaptation almost exclusively by agents who hold higher places in the global wealth distribution. This occurs because the

barriers to international migration are large enough such that many poor agents find it too expensive to adapt through the migration channel and instead are forced to rely solely on self-insurance. The inequitable access to migration as adaptation leads to the effects of climate change at the individual level to be highly unequal across poor and rich agents. While the aggregate effects of climate change on welfare under RCP4.5 are near-zero, poor agents' welfare declines by over 8.5 percent while the richest agents experience welfare gains of between 3 and 5 percent.

The broad prediction of both the simple and calibrated models is that the value of international migration as adaptation will depend crucially on its financial costs. Forcing that agents pay a real cost – beyond pure disutility alone – in order to migrate reflects the reality that migration, even net of physical travel costs, is not costless in the real world. This leads to sharp nonlinearities in the modeled migration policy functions, a feature absent from existing state-of-the art regional macroeconomic models of climate change. These nonlinearities capture observed features of migration where, for poor countries, emigration is increasing in income (Cai et al. 2016; Barbosa Alves and Braulio 2023). If future barriers to migration manifest as monetary costs as well as disutility, the model strongly suggests we should expect to see stark differences between the effects of climate change on agents who can afford to migrate and those who cannot.

This first step in bridging the gap between the neoclassical and spatial approaches (Krusell and Smith 2022; Cruz and Rossi-Hansberg 2023) suggests that agents' behavior when they have access to adaptation across space and time may not resemble a convex combination of the outcomes that would occur when each channel is accessible in isolation. My combination of the two approaches is not without drawbacks; the model here lets go of a number of attractive features unique to the above models, including making climate change and energy use endogenous, allowing for incompleteness in global capital markets, and accounting for the twin effects of crowding and agglomeration when considering how agents select locations. Other simplifying assumptions lead the model to over-predict the appeal of small countries in the global north which causes the model to underestimate the number of agents who are negatively affected by climate change. Nevertheless, the preliminary work here suggests that future work on spatial models of climate change that characterizes how income heterogeneity shapes individual-level adaptation decisions promises new insights into how they will affect global aggregates.

References

- Abel, Guy J, and Joel E Cohen. 2022. “Bilateral international migration flow estimates updated and refined by sex”. *Scientific Data* 9 (1): 173. (Cit. on pp. 12, 25).
- Acemoglu, Daron. 2008. *Introduction to modern economic growth*. Princeton university press. (Cit. on p. 24).
- Acemoglu, Daron, and Martin Kaae Jensen. 2015. “Robust comparative statics in large dynamic economies”. *Journal of Political Economy* 123 (3): 587–640. (Cit. on p. A.14).
- Aiyagari, S Rao. 1994. “Uninsured idiosyncratic risk and aggregate saving”. *The Quarterly Journal of Economics* 109 (3): 659–684. (Cit. on pp. 2, 15, 20).
- Aiyagari, S Rao, and Ellen R McGrattan. 1998. “The optimum quantity of debt”. *Journal of Monetary Economics* 42 (3): 447–469.
- Alsina-Pujols, Maria. 2021. “Warming with borders: climate refugees and carbon pricing”. (Cit. on p. 1).
- Barbosa Alves, Mauricio, and Britosm Braulio. 2023. “Climate Change and International Migration”. (Cit. on pp. 2, 7, 20, 42).
- Barrage, Lint, and William Nordhaus. 2024. “Policies, projections, and the social cost of carbon: Results from the DICE-2023 model”. *Proceedings of the National Academy of Sciences* 121 (13): e2312030121. (Cit. on p. 6).
- Bazzi, Samuel. 2017. “Wealth heterogeneity and the income elasticity of migration”. *American Economic Journal: Applied Economics* 9 (2): 219–255. (Cit. on pp. 2, 3, 13, 20, 21, 28, 41).
- Benveniste, Hélène, Michael Oppenheimer, and Marc Fleurbaey. 2022. “Climate change increases resource-constrained international immobility”. *Nature Climate Change* 12 (7): 634–641.
- Bilal, Adrien, and Esteban Rossi-Hansberg. 2023. *Anticipating Climate Change Across the United States*. Tech. rep. National Bureau of Economic Research. (Cit. on pp. 4, 7, 14, 37).
- Burzyński, Michał, et al. 2022. “Climate change, inequality, and human migration”. *Journal of the European Economic Association* 20 (3): 1145–1197. (Cit. on p. 6).
- Cai, Ruohong, et al. 2016. “Climate variability and international migration: The importance of the agricultural linkage”. *Journal of Environmental Economics and Management* 79:135–151. (Cit. on pp. 2, 21, 42).

- Cai, Shu. 2020. "Migration under liquidity constraints: Evidence from randomized credit access in China". *Journal of Development Economics* 142:102247. (Cit. on pp. 2, 3, 13, 21, 41).
- Carroll, Christopher D. 2006. "The method of endogenous gridpoints for solving dynamic stochastic optimization problems". *Economics letters* 91 (3): 312–320. (Cit. on p. A.14).
- CIESIN, Center for International Earth Science Information Network. 2017. "Gridded Population of the World, Version 4 (GPWv4): Population Count, Revision 10". *Atlas of Environmental Risks Facing China Under Climate Change*. Visited on 03/01/2024. <https://doi.org/10.7927/H4PG1PPM>. (Cit. on p. 22).
- Clemens, Michael A, Claudio E Montenegro, and Lant Pritchett. 2019. "The place premium: Bounding the price equivalent of migration barriers". *Review of Economics and Statistics* 101 (2): 201–213. (Cit. on pp. 3, 12, 21, 24, 28, 41).
- Colmer, Jonathan. 2021. "Temperature, labor reallocation, and industrial production: Evidence from India". *American Economic Journal: Applied Economics* 13 (4): 101–124. (Cit. on p. 20).
- Conesa, Juan C, and Dirk Krueger. 1999. "Social security reform with heterogeneous agents". *Review of Economic dynamics* 2 (4): 757–795. (Cit. on pp. 32, 35).
- Conte, Bruno, et al. 2021. "Local sectoral specialization in a warming world". *Journal of Economic Geography* 21 (4): 493–530. (Cit. on p. 6).
- Cruz, José-Luis, and Esteban Rossi-Hansberg. 2023. "The Economic Geography of Global Warming". *Review of Economic Studies*: rdad042. (Cit. on pp. 1, 2, 5–7, 12, 14, 34, 42).
- Cruz, José-Luiz. 2023. "Global Warming and Labor Market Reallocation". (Cit. on pp. 1, 5, 6).
- Desmet, Klaus, Dávid Krisztián Nagy, and Esteban Rossi-Hansberg. 2018. "The geography of development". *Journal of Political Economy* 126 (3): 903–983. (Cit. on p. 7).
- Desmet, Klaus, and Esteban Rossi-Hansberg. 2024. "Climate Change Economics over Time and Space". *University of Chicago, Becker Friedman Institute for Economics Working Paper*: 2024–25. (Cit. on pp. 1, 7).
- . 2015. "On the spatial economic impact of global warming". *Journal of Urban Economics* 88:16–37. (Cit. on p. 6).
- Eyring, Veronika, et al. 2016. "Overview of the Coupled Model Intercomparison Project Phase 6 (CMIP6) experimental design and organization". *Geoscientific Model Development* 9 (5): 1937–1958. (Cit. on pp. 3, 22, 32).

- Feenstra, Robert C, Robert Inklaar, and Marcel P Timmer. 2015. “The next generation of the Penn World Table”. *American economic review* 105 (10): 3150–3182. (Cit. on pp. A.15, A.17).
- GADM. 2022. “GADM database of global administrative areas v4.1”. <https://gadm.org/data.html>. (Cit. on p. 22).
- Golosov, Mikhail, et al. 2014. “Optimal taxes on fossil fuel in general equilibrium”. *Econometrica* 82 (1): 41–88. (Cit. on p. 24).
- Gröger, André, and Yanos Zylberberg. 2016. “Internal labor migration as a shock coping strategy: Evidence from a typhoon”. *American Economic Journal: Applied Economics* 8 (2): 123–153. (Cit. on p. 20).
- Grogger, Jeffrey, and Gordon H Hanson. 2011. “Income maximization and the selection and sorting of international migrants”. *Journal of Development Economics* 95 (1): 42–57. (Cit. on p. 12).
- Hoffmann, Roman, et al. 2020. “A meta-analysis of country-level studies on environmental change and migration”. *Nature Climate Change* 10 (10): 904–912. (Cit. on p. 1).
- Hopenhayn, Hugo A, and Edward C Prescott. 1992. “Stochastic monotonicity and stationary distributions for dynamic economies”. *Econometrica: Journal of the Econometric Society*: 1387–1406. (Cit. on p. A.14).
- Hsiang, Solomon M, Kyle C Meng, and Mark A Cane. 2011. “Civil conflicts are associated with the global climate”. *Nature* 476 (7361): 438–441. (Cit. on p. 30).
- Iskhakov, Fedor, et al. 2017. “The endogenous grid method for discrete-continuous dynamic choice models with (or without) taste shocks”. *Quantitative Economics* 8 (2): 317–365. (Cit. on pp. 10, 20, A.13, A.14).
- Krusell, Per, and Anthony Smith. 2022. *Climate change around the world*. Tech. rep. National Bureau of Economic Research. (Cit. on pp. 1, 6, 7, 24, 42).
- Lagakos, David, Ahmed Mushfiq Mobarak, and Michael E Waugh. 2023. “The welfare effects of encouraging rural–urban migration”. *Econometrica* 91 (3): 803–837. (Cit. on pp. 12, 13, 21, 23, 24).
- Lee, June-Yi, et al. 2021. “Future global climate: scenario-based projections and near-term information”. In *Climate change 2021: The physical science basis. Contribution of working group I to the sixth assessment report of the intergovernmental panel on climate change*, 553–672. Cambridge University Press. (Cit. on p. 22).

- Liu, Maggie, Yogita Shamdasani, and Vis Taraz. 2023. “Climate change and labor reallocation: Evidence from six decades of the Indian Census”. *American Economic Journal: Economic Policy* 15 (2): 395–423. (Cit. on p. 1).
- Nath, Ishan B. 2020. *The Food Problem and the Aggregate Productivity Consequences of Climate Change*. Tech. rep. National Bureau of Economic Research. (Cit. on p. 6).
- Nath, Ishan B, Valerie A Ramey, and Peter J Klenow. 2023. *How Much Will Global Warming Cool Global Growth?* Tech. rep. Working paper. (Cit. on pp. 1, 3, 22, 33).
- Nordhaus, William D. 1992. “An optimal transition path for controlling greenhouse gases”. *Science* 258 (5086): 1315–1319. (Cit. on p. 6).
- Nordhaus, William D. 2010. “Economic aspects of global warming in a post-Copenhagen environment”. *Proceedings of the National Academy of Sciences* 107 (26): 11721–11726. (Cit. on p. 6).
- Nordhaus, William D., and Zili Yang. 1996. “A regional dynamic general-equilibrium model of alternative climate-change strategies”. *American Economic Review*: 741–765. (Cit. on p. 6).
- Piketty, Thomas. 2014. *Capital in the twenty-first century*. Harvard University Press. (Cit. on p. 24).
- Recchi, Ettore, et al. 2021. “The global visa cost divide: How and why the price for travel permits varies worldwide”. *Political Geography* 86:102350. (Cit. on pp. 2, 15).
- Rudik, Ivan, et al. 2021. *Heterogeneity and Market Adaptation to Climate Change in Dynamic-Spatial Equilibrium*. Tech. rep. Iowa State University, Department of Economics. (Cit. on p. 6).
- Rust, John. 1987. “Optimal replacement of GMC bus engines: An empirical model of Harold Zurcher”. *Econometrica: Journal of the Econometric Society*: 999–1033. (Cit. on p. 18).
- Schwalm, Christopher R, Spencer Glendon, and Philip B Duffy. 2020. “RCP8. 5 tracks cumulative CO₂ emissions”. *Proceedings of the National Academy of Sciences* 117 (33): 19656–19657. (Cit. on p. 32).
- Shimer, Robert. 2005. “The cyclical behavior of equilibrium unemployment and vacancies”. *American economic review* 95 (1): 25–49. (Cit. on pp. 23, 24).
- Surak, Kristin. 2021. “Millionaire mobility and the sale of citizenship”. *Journal of Ethnic and Migration Studies* 47 (1): 166–189. (Cit. on pp. 2, 15).
- Train, Kenneth E. 2009. *Discrete choice methods with simulation*. Cambridge university press. (Cit. on p. 10).

- Uhlig, Harald. 1996. “A law of large numbers for large economies”. *Economic Theory* 8:41–50. (Cit. on p. 19).
- Van Vuuren, Detlef P, et al. 2011. “The representative concentration pathways: an overview”. *Climatic change* 109:5–31. (Cit. on p. 22).
- Vince, Gaia. 2022. *Nomad century: how climate migration will reshape our world*. Flatiron Books. (Cit. on pp. 4, 40, 41).
- Walsh, Kieran J., and Eric R Young. 2024. *Equilibrium Multiplicity in Aiyagari and Krusell-Smith*. Tech. rep. (Cit. on pp. 20, A.14).
- WBG. 2016. *World development indicators 2016*. The World Bank. (Cit. on pp. 21, 28).
- Yang, Zili. 2023. “The Model Dimensionality and Its Impacts on the Strategic and Policy Outcomes in IAMs the Findings from the RICE2020 Model”. *Computational Economics* 62 (3): 1087–1106. (Cit. on pp. 1, 6).

Appendix

Contents

A Proof of Proposition 1	A.2
B Proof of Proposition 2	A.3
C Proof of Existence for an Equilibrium in the Toy Model	A.5
D Ambiguity in the General Case	A.7
E Proof of Ambiguity Under a Unique Equilibrium	A.9
F The Numerical Solution for the Calibrated Model	A.12
G Venezuela and Colombia	A.15
G.1 Initial Equilibrium	A.16
G.2 Modeling post-2013 Venezuela	A.17
G.3 Modeled Transition Path	A.19
H Solving for Transition Paths	A.21
H.1 Solution Algorithm	A.21
H.2 Average Welfare Losses by Wealth Decile	A.23
I Steady-State Warming and Productivity Changes under RCP8.5	A.24

A Proof of Proposition 1

Proof. Part 1: An increase in m raises $\pi(i, i)$.

Consider the expression for $\pi(i, i)$:

$$\pi(i, i) = \frac{1}{\int_0^1 e^{W(i,j)-W(i,i)} dj} \quad (\text{A.1})$$

Substituting for each $W(i, j)$, the optimal savings policy $S^*(i, j)$ from the agents' Euler equations is

$$\begin{aligned} \frac{1 - \beta}{y - m(i, j) - S(i, j)} &= \frac{\beta R}{w_2(j) + RS(i, j)} \\ S^*(i, j) &= \frac{\beta R(y - m(i, j)) - (1 - \beta)w_2(j)}{R} \end{aligned} \quad (\text{A.2})$$

where $R = (1 + r)$ is the gross return to savings. $W(i, j)$ is then equal to

$$W(i, j) = \ln \left(\frac{\left((1 - \beta)R(y - m(i, j)) + (1 - \beta)w_2(j) \right)^{1-\beta}}{\left(\beta R(y - m(i, j)) + \beta w_2(j) \right)^{-\beta}} \right)$$

and $W(i, j) - W(i, i)$ becomes:

$$W(i, j) - W(i, i) = \ln \left(\frac{R(y - m(i, j)) + w_2(j)}{Ry + w_2(i)} \right) \quad (\text{A.3})$$

Substitute for the $W(i, j) - W(i, i)$ terms in Equation (A.1) and differentiate in m

$$d\pi(i, i) = \frac{\left[-\pi(i, i) \frac{\partial}{\partial m} \left\{ \int_0^1 R(y - m(i, j)) + w_2(j) dj \right\} \right]}{\int_0^1 R(y - m(i, j)) + w_2(j) dj} dm \quad (\text{A.4})$$

such that

$$\frac{\partial m(i, j)}{\partial m} > 0, \quad \forall i \neq j$$

and

$$\frac{\partial m(i, i)}{\partial m} = 0$$

Rearranging and noting that the denominator on the large bracketed term is positive implies

$$\frac{d\pi(i, i)}{dm} \propto -\pi(i, i) \frac{\partial}{\partial m} \left\{ \int_0^1 R(y - m(i, j)) + w_2(j) dj \right\} \quad (\text{A.5})$$

Applying Leibniz's integral rule leaves

$$\frac{d\pi(i, i)}{dm} \propto \left[\pi(i, i) \left\{ \int_0^1 Rm'(i, j) dj \right\} \right] > 0 \quad (\text{A.6})$$

Part 2: A decline in $A_2(j)$ lowers $\pi(i, j)$.

Starting with $\pi(i, j)$ and taking its derivative in $A_2(i)$ gives:

$$\frac{d\pi(i, j)}{dA_2(j)} = \frac{\left[\tilde{w} - \pi(i, j) \frac{\partial}{\partial A_2(j)} \left\{ \int_0^1 R(y - m(i, k)) + w_2(k) dk \right\} \right]}{\int_0^1 R(y - m(i, k)) + w_2(k) dk}$$

where

$$\tilde{w} = (1 - \alpha) \left(\frac{\alpha}{r} \right)^{\frac{\alpha}{1-\alpha}}$$

is the wage per effective worker. As the denominator is positive, applying Leibniz's rule and rearranging gives the desired result

$$\frac{d\pi(i, j)}{dA_2(j)} \propto \left[\tilde{w}(1 - \pi(i, j)) \right] > 0 \quad (\text{A.7})$$

as $\pi(i, j) < 1$.

□

B Proof of Proposition 2

Proof. Differentiating Equation (A.1) in r gives

$$d\pi(i, i) = \frac{[y - A_2(i)\tilde{w}'(r) - \pi(i, i)\frac{\partial}{\partial r} \left\{ \int_0^1 R(y - m(i, j)) + w_2(j) dj \right\}]}{\int_0^1 R(y - m(i, j)) + w_2(j) dj} dr \quad (\text{B.1})$$

where

$$\tilde{w}'(r) = -\alpha \left(\frac{\alpha}{r} \right)^{\frac{1}{1-\alpha}} < 0$$

is the change of effective wages with the interest rate offered to firms. The sign of this derivative is determined by

$$\frac{d\pi(i, i)}{dr} \propto (y - A_2(i)\tilde{w}'(r)) - \pi(i, i)\frac{\partial}{\partial r} \left\{ \int_0^1 R(y - m(i, j)) + w_2(j) dj \right\} \quad (\text{B.2})$$

Applying Leibniz's integral rule leaves

$$\frac{d\pi(i, i)}{dr} \propto y(1 - \pi(i, i)) + \pi(i, i)\overline{m(j)} + \tilde{w}'(r)(\pi(i, i)\bar{A} - A_2(i)) \quad (\text{B.3})$$

where in the last line the terms \bar{A} and $\overline{m(j)}$ denote the arithmetic mean of second-period productivity and travel costs across each island j that receives a nonzero share of agents from island i in the second period. That is

$$\bar{A} = \int_{\mathcal{J}} A_2(j) dj \quad \overline{m(j)} = \int_{\mathcal{J}} m(i, j) dj$$

where

$$\mathcal{J} = \left\{ j \in [0, 1] : \beta R(y - m(i, j)) + \beta w_2(j) > 0 \right\}$$

As $\tilde{w}'(r) < 0$, the second term in the line above can be signed only if island i has higher productivity than \bar{A} in which case all terms are positive. Otherwise, the effect of increasing the returns to savings on the share of agents who stay on a given island is ambiguous.

□

C Proof of Existence for an Equilibrium in the Toy Model

Proof. To prove at least one equilibrium in this economy exists requires finding an interest rate at which equation (4) holds when both aggregate demand and supply of capital are generated by the optimal policies of agents and firms at interest rate r . A sufficient condition for existence of an equilibrium is that the excess demand function for capital (that is, aggregate demand less supply as a function of r) is continuous and its codomain includes values both above and below zero. I show that (1) aggregate capital supply and demand are continuous on $r \in (0, \infty)$ and (2) the interval created by the limiting values of the excess demand function evaluated as $r \rightarrow 0^+$ and $r \rightarrow \infty$ contains zero.

Proving (1): Showing aggregate supply and demand are differentiable on $r \in (0, \infty)$ is sufficient for the continuity of the excess demand function for capital as the sum of two continuous functions is continuous. Letting R again denote the gross interest rate, aggregate capital demand is

$$\begin{aligned} K^D(r) &= \left(\frac{\alpha}{r}\right)^{\frac{\alpha}{1-\alpha}} \left(\int_0^1 A(i) N_2(i) di \right) \\ &= \left(\frac{\alpha}{r}\right)^{\frac{\alpha}{1-\alpha}} \left(\int_0^1 A(i) \int_0^1 \pi(j, i) dj di \right) \\ &= \left(\frac{\alpha}{r}\right)^{\frac{\alpha}{1-\alpha}} \left(\int_0^1 A(i) \int_0^1 \left[\frac{R(y - m(j, i)) + w_2(i)}{\int R(y - m(j, k)) + w_2(k) dk} \right] dj di \right) \\ &= \left(\frac{\alpha}{r}\right)^{\frac{\alpha}{1-\alpha}} \left(\int_0^1 A(i) \int_0^1 \left[\frac{R(y - m(j, i)) + \tilde{w}(r) A(i)}{R(y - \overline{m(j)}) + \tilde{w}(r) \bar{A}} \right] dj di \right) \end{aligned}$$

where in the last line the terms \bar{A} and $\overline{m(j)}$ are defined above in Proposition 2. Differentiating $K^D(r)$ in r and applying Leibniz's integral rule gives

$$\frac{\partial K^D(r)}{\partial r} = \underbrace{- \left(\frac{\alpha^2}{(1-\alpha)r} \right) K^D(r)}_{\text{PE}} + \underbrace{\left(\frac{\alpha}{r} \right)^{\frac{\alpha}{1-\alpha}} \left(\int_0^1 A(i) \int_0^1 \frac{\partial \pi(j, i)}{\partial r} dj di \right)}_{\text{GE}}$$

The partial equilibrium (PE) effect of increasing the rental rate r is naturally negative. The integrand of the second term (the general equilibrium effect) is²⁵

²⁵Strictly speaking this is a misnomer as a change in interest rates would affect agents' second-period choices for locations even in the absence of secondary effects on wages. I find the label convenient to

$$\frac{\partial \pi(j, i)}{\partial r} = \frac{1}{R(y - \bar{m}(j)) + \tilde{w}(r)\bar{A}} \left[(y - m(j, i)) + \tilde{w}'(r)A(i) - \pi(j, i) \left((y - \bar{m}(j)) + \tilde{w}'(r)\bar{A} \right) \right] \quad (\text{C.1})$$

where again

$$\tilde{w}'(r) = -\alpha \left(\frac{\alpha}{r} \right)^{\frac{1}{1-\alpha}} < 0$$

As agents only choose second period locations that give positive consumption each period, the denominator in equation (C.1) is positive on the open interval $r \in (0, \infty)$ as it is an average of second period consumption for agents who start on island i . The partial in (C.1) is then well-defined for all (i, j) and $K^D(r)$ is continuous. For capital supply, we have:

$$K^S(r) = \int_0^1 \int_0^1 \pi(i, j) S(i, j) dj di$$

Differentiating in r and applying Leibniz' rule gives:

$$\frac{\partial K^S(r)}{\partial r} = \int_0^1 \int_0^1 \underbrace{\frac{\partial \pi(i, j)}{\partial r} S(i, j)}_{\text{GE}} + \underbrace{\frac{\partial S(i, j)}{\partial r} \pi(i, j)}_{\text{PE}} dj di$$

We have already shown the general equilibrium effects portion (the GE term) of this derivative is well-defined. As the savings function is continuous The partial equilibrium (PE) effect of changes in the interest rate on savings $S(i, j)$

$$\frac{\partial S(i, j)}{\partial r} = \frac{(1 - \beta)[\tilde{w}(r)A(j) - R\tilde{w}'(r)A_j]}{R^2} \quad (\text{C.2})$$

is also well-defined for all $r \in (0, \infty)$ across all i, j pairs. This shows that both capital demand and supply are differentiable in r on the interval $(0, \infty)$, which ensures the excess demand function is continuous on this interval.

Proving (2): The limiting values for capital supply on the open interval $r \in (0, \infty)$ are

differentiate effects on what might more-accurately be described as intensive and extensive margins.

$$\lim_{r \rightarrow \infty} K^S(r) = \left(\beta \int_0^1 \int_0^1 \pi(i, j)(y - m(i, j)) dj di \right) > 0$$

and

$$\lim_{r \rightarrow 0^+} K^S(r) = - \int_0^1 \int_0^1 \pi(i, j)(1 - \beta)\tilde{w}(r)A(j) dj di = -\infty$$

by

$$\lim_{r \rightarrow 0^+} \tilde{w}(r) = \infty$$

The limiting values for demand are

$$\lim_{r \rightarrow \infty} K^D(r) = 0$$

$$\lim_{r \rightarrow 0^+} K^D(r) = \infty$$

The excess demand function

$$Z(r) = K^D(r) - K^S(r, w)$$

then tends to positive infinity as $r \rightarrow 0$ and tends to

$$\lim_{r \rightarrow \infty} Z(r) = - \lim_{r \rightarrow \infty} K^S(r, w) < 0$$

as $r \rightarrow \infty$. As $Z(r)$ is the sum of two differentiable functions on $(0, \infty)$ it is also differentiable and continuous. By the Intermediate Value Theorem, $Z(r)$ must equal zero (such that supply and demand are equal) at least once on the open interval $r \in (0, \infty)$. \square

D Ambiguity in the General Case

Proof. Part 1: Start again with the function characterizing how the share of stayers $\pi(i, i)$ changes in m from equation (A.4) of Appendix A.

$$\frac{d\pi(i, i)}{dm} = \frac{\left[\frac{\partial r}{\partial m} (y + A_2(i)w'(r)) - \pi(i, i) \frac{\partial}{\partial m} \left\{ \int_0^1 R(y - m(i, j)) + w_2(j) dj \right\} \right]}{\int_0^1 R(y - m(i, j)) + w_2(j) dj}$$

Again noting that the denominator on the large bracketed term is positive leaves

$$\frac{d\pi(i, i)}{dm} \propto \left[\frac{\partial r}{\partial m} (y + A_2(i)w'(r)) - \pi(i, i) \frac{\partial}{\partial m} \left\{ \int_0^1 R(y - m(i, j)) + w_2(j) dj \right\} \right]$$

Applying Leibniz's rule

$$\frac{d\pi(i, i)}{dm} \propto \frac{\partial r}{\partial m} (y + A_2(i)\tilde{w}'(r)) - \pi(i, i) \left\{ \int_0^1 \frac{\partial r}{\partial m} (y - m(i, j) + A_2(j)\tilde{w}'(r)) - Rm'(i, j) dj \right\}$$

Evaluating the integral and combining like terms

$$\begin{aligned} \frac{d\pi(i, i)}{dm} &\propto \frac{\partial r}{\partial m} (y + A_2(i)\tilde{w}'(r)) - \pi(i, i) \left(\frac{\partial r}{\partial m} (y - \overline{m(i)} + \overline{A}\tilde{w}'(r)) - R\overline{m'(i)} \right) \\ &\propto \frac{\partial r}{\partial m} \left(y(1 - \pi(i, i)) + \pi(i, i)\overline{m(i)} + \tilde{w}'(r)(A_2(i) - \overline{A}\pi(i, i)) \right) + \pi(i, i)R\overline{m'(i)} \leq 0 \end{aligned}$$

As the sign of the large parenthetical terms as well as $\frac{\partial r}{\partial m}$ are unknown, the effects of increasing migration costs on $\pi(i, i)$ are ambiguous.

Part 2: Starting from the formula for $\pi(j, i)$ in the main text, differentiate in $A_2(i)$:

$$\frac{d\pi(j, i)}{dA_2(i)} = \frac{\left[\frac{\partial r}{\partial A_2(i)} (y - m(j, i) + A_2(i)\tilde{w}'(r)) + \tilde{w}(r) - \pi(j, i) \frac{\partial}{\partial A_2(i)} \left\{ \int_0^1 R(y - m(j, k)) + w_2(k) dk \right\} \right]}{\int_0^1 R(y - m(j, k)) + w_2(k) dk}$$

Again noting that the denominator is positive and applying Leibniz's rule leaves

$$\begin{aligned} \frac{d\pi(j, i)}{dA_2(i)} &\propto \frac{\partial r}{\partial A_2(i)} (y - m(j, i) + A_2(i)\tilde{w}'(r)) + \tilde{w}(r) \\ &\quad - \pi(j, i) \frac{\partial r}{\partial A_2(i)} \left\{ \int_0^1 R(y - m(j, k)) + A_2(k)\tilde{w}(r) dk \right\} \end{aligned}$$

$$\begin{aligned} \frac{d\pi(j, i)}{dA_2(i)} &\propto \frac{\partial r}{\partial A_2(i)} \left(y(1 - \pi(j, i)) - m(j, i) + \pi(j, i)\overline{m(i)} \right. \\ &\quad \left. + \tilde{w}'(r)(A_2(i) - \overline{A}\pi(j, i)) \right) + \tilde{w}(r)(1 - \pi(j, i)) \leq 0 \end{aligned}$$

As the sign of both $\frac{\partial r}{\partial A_2(i)}$ and the large parenthetical are again unknown, the effects of a

decrease in $A_2(i)$ on $\pi(i, i)$ are ambiguous.

□

E Proof of Ambiguity Under a Unique Equilibrium

Proof. We seek to show that the effects of a change in m on r and implicitly $\pi(i, i)$ are indeterminate even in the case of unique equilibria. Following from Appendix C, let

$$Z(r, \Theta) = K^D(r, \Theta) - K^S(r, \Theta) = 0$$

be the excess demand function for capital in an equilibrium where exogenous parameters $\{m, \{A_2\}, \alpha, \beta\}$ are summarized by Θ . Taking its total derivative in Θ and setting all changes less dm to zero gives

$$\nabla Z \cdot d\Theta = 0 = \frac{\partial K^D(r, \Theta)}{\partial m} dm - \frac{\partial K^S(r, \Theta)}{\partial m} dm + \frac{\partial K^D(r, \Theta)}{\partial r} dr - \frac{\partial K^S(r, \Theta)}{\partial r} dr$$

For the capital demand portion of excess demand, we have

$$\frac{\partial K^D(r, \Theta)}{\partial m} = \frac{\partial}{\partial m} \left(\frac{\alpha}{r} \right)^{\frac{\alpha}{1-\alpha}} \left(\int_0^1 \int_0^1 A(i) \pi(j, i) dj di \right) + \frac{\partial K^D(r)}{\partial r} \frac{dr}{dm} \quad (\text{E.1})$$

where the partial derivative of K^D in r is as-described in Appendix C. An analogous expression for the supply term is

$$\frac{\partial K^S(r, \Theta)}{\partial m} = \frac{\partial}{\partial m} \left(\int_0^1 \int_0^1 \pi(j, i) S(j, i) dj di \right) + \frac{\partial K^S(r, \Theta)}{\partial r} \frac{dr}{dm} \quad (\text{E.2})$$

In the case of a unique equilibrium where both the capital supply and demand functions are monotonic, we have that

$$\frac{\partial K^D(r)}{\partial r} < 0$$

and

$$\frac{\partial K^S(r)}{\partial r} > 0$$

on the open interval $r \in (0, \infty)$. To rule out ambiguity in the effects of changes in m on the equilibrium interest rate, we must sign the other two terms in equations (E.1) and (E.2)

above. Beginning with the capital demand term, we may re-write the first term as

$$\frac{\partial}{\partial m} \left(\frac{\alpha}{r} \right)^{\frac{\alpha}{1-\alpha}} \left(\int_0^1 \int_0^1 A(i) \pi(j, i) dj di \right) = \left(\frac{\alpha}{r} \right)^{\frac{\alpha}{1-\alpha}} \frac{\partial}{\partial m} \left(\text{cov}(A(i), \pi(j, i)) + \mathbb{E}[A(i)] \mathbb{E}[\pi(j, i)] \right) \quad (\text{E.3})$$

by applying the definition of covariance. Applying the chain rule and Leibniz's rule on the second term

$$\begin{aligned} \frac{\partial}{\partial m} (\mathbb{E}[A(i)] \mathbb{E}[\pi(j, i)]) &= \mathbb{E}[A(i)] \frac{\partial}{\partial m} \mathbb{E}[\pi(j, i)] + \frac{\partial}{\partial m} \mathbb{E}[A(i)] \mathbb{E}[\pi(j, i)] \\ &= \mathbb{E}[A(i)] \int_0^1 \int_0^1 \frac{\partial}{\partial m} \pi(j, i) dj di + (0) \mathbb{E}[\pi(j, i)] = 0 \end{aligned}$$

As the integral over all changes in migration shares must be equal to zero. This leaves

$$\frac{\partial K^D(r, \Theta)}{\partial m} = \left(\frac{\alpha}{r} \right)^{\frac{\alpha}{1-\alpha}} \frac{\partial}{\partial m} \left(\text{cov}(A(i), \pi(j, i)) \right) + \frac{\partial K^D(r)}{\partial r} \frac{dr}{dm}$$

Applying an analogous argument to the firm term in equation (E.2) governing changes in capital supply leaves:

$$\frac{\partial K^S(r, \Theta)}{\partial m} = \frac{\partial}{\partial m} \left(\text{cov}(S(i, j), \pi(i, j)) \right) + \mathbb{E}[\pi(i, j)] \int_0^1 \int_0^1 \frac{\partial}{\partial m} S(i, j) di dj + \frac{\partial K^S(r, \Theta)}{\partial r} \frac{dr}{dm}$$

Note the partial derivative of expected savings

$$\frac{\partial}{\partial m} S(i, j) = \frac{\partial}{\partial m} \frac{\beta R(y - m(i, j)) - (1 - \beta) w_2(j)}{R} \leq 0$$

is non-positive for all pairs and negative when $i \neq j$. Taking stock, we have that the only unsigned terms remaining in the total derivative of the capital demand equation (outside of $\frac{dr}{dm}$) are the two covariance terms:

$$\frac{dZ}{dm} = 0 = \left(\frac{\alpha}{r}\right)^{\frac{\alpha}{1-\alpha}} \frac{\partial}{\partial m} \left(\text{cov}(A(i), \pi(j, i)) \right) - \frac{\partial}{\partial m} \left(\text{cov}(S(i, j), \pi(i, j)) \right)$$

$$+ \underbrace{\mathbb{E}[\pi(i, j)] \int_0^1 \int_0^1 \frac{\partial}{\partial m} S(i, j) di dj}_{<0} + \underbrace{\left(\frac{\partial K^D(r)}{\partial r} - \frac{\partial K^S(r, \Theta)}{\partial r} \right) \frac{dr}{dm}}_{<0}$$

The only case where the direction of $\frac{dr}{dm}$ can be known is where

$$\frac{\partial}{\partial m} \left[\text{cov}(A(i), \pi(j, i)) \right] < 0$$

and

$$\frac{\partial}{\partial m} \left[\text{cov}(S(i, j), \pi(i, j)) \right] > 0$$

In this narrow case, all terms are signed and we may guarantee that

$$\frac{dr}{dm} < 0$$

I argue this is unlikely to hold generally. For the first covariance term in the equation for capital demand, consider $\text{cov}(A(i), \pi(j, i))$ as $m(i, j) \rightarrow \infty$ for all $i \neq j$. When $m(i, j)$ is sufficiently large, $\pi(i, j)$ will be equal to zero for all $i \neq j$ which implies:

$$\lim_{m \rightarrow \infty} \text{cov}(A(i), \pi(j, i)) = 0$$

In the contrasting case where $m = 0$, we have

$$\pi(i, j) = \frac{Ry + w_2(j)}{\int_0^1 Ry + w_2(k) dk} = \frac{Ry + \tilde{w} A_2(j)}{Ry + \tilde{w} \bar{A}}$$

Holding the average productivity level across all islands in the second period \bar{A} fixed, $\pi(i, j)$ is increasing in $A(j)$ for all origins i . Thus this covariance at $m = 0$ is positive. If the derivative in (E.3) is continuous then this first covariance term should indeed be decreasing in m at some point. However, we cannot guarantee that this derivative is monotonically decreasing in m . Examining the second covariance term, again as $m \rightarrow \infty$ we have

$$\lim_{m \rightarrow \infty} \text{cov}(S(i, j), \pi(i, j)) = 0$$

by a similar argument as above. As $m \rightarrow 0$, we have

$$S(i, j) = \frac{\beta Ry - (1 - \beta)\tilde{w}A_2(j)}{R}$$

When $m = 0$, the savings function from any initial location is strictly decreasing in the productivity on their destination island. As shown above, in contrast to this we have that $\pi(i, j)$ is increasing in $A_2(j)$. Thus the covariance between savings and emigration shares is negative when $m = 0$. If we again impose continuity on the derivative in (E.3) then we should have at some point that the second covariance term is increasing in m . However, like with the first covariance term even under continuity we cannot guarantee this derivative is monotonic.

□

F The Numerical Solution for the Calibrated Model

I solve for the SRCE associated with a given set of structural parameters Θ using value function iteration (VFI) through implementing the following algorithm:

1. Initialize a grid of potential equilibrium interest rates in the interval $r \in [\underline{r}, \bar{r}]$ where $\bar{r} < \frac{\gamma}{\beta}$ and $\underline{r} > 0$.
2. Initialize a guess for the expected value functions $\mathbb{E}[\hat{V}^n(\hat{x}, \hat{d})|r] = \mathbf{0}$ indexed at $n = 1$ for each candidate interest rate r .
3. Update the conditional value functions using

$$\mathbb{E}[\hat{V}^{n+1}(\hat{x}, \hat{d})|r] = T(\mathbb{E}[\hat{V}^n(\hat{x}, \hat{d})|r]) \quad (\text{F.1})$$

where $T(\mathbb{E}[V_t(\cdot)|r])$ is the operator defined on the right-hand side of equation (9):

$$T(\mathbb{E}[\hat{V}^n(\hat{x}, \hat{d})]) = \sum_{s' \in \ell, h} \Pi_{ss'} \ln \left(\sum_{k_{t+1}} \exp \left(\max_{\hat{a}' \in \Gamma(x')} \left\{ u(x', d') + \beta \mathbb{E}[\hat{V}^n(x', d')] \right\} \right) \right)$$

4. Iterate on the operator until it converges in the sup norm within tolerance tol .

$$\sup_{\hat{x}, \hat{d}} \left\| \mathbb{E}[\hat{V}^{n+1}(\hat{x}, \hat{d})|r] - \mathbb{E}[\hat{V}^n(\hat{x}, \hat{d})|r] \right\| < tol$$

5. Solve for the resulting CCPs $\pi(\hat{x}, j|r)$ induced by the conditional value functions $\mathbb{E}[V_t(\cdot)|r]$.
6. Initialize a large number of agents ($N = 200,000$) with random values for \hat{x}, \hat{d} in an initial period, sample labor endowment processes for each agent from the Markov process Π and draw a set of taste shocks for each agent each period, and simulate location choices and asset holdings forward for each value of r for 500 periods for each agent.
7. When distribution has settled, solve for $K^D(r)$ and aggregate savings.
8. Find the two interest rates r^-, r^+ in the grid where

$$\underbrace{\sum_{h=1}^N \hat{K}_h^D(r)}_{\text{aggregate demand}} - \underbrace{\sum_{\hat{x}} \hat{\Omega}(\hat{x}|r) \sum_{j=1}^N g(\hat{x}, j|r) \pi(\hat{x}, j|r)}_{\text{aggregate savings}}$$

is closest to zero

9. If the distance $|r^- - r^+|$ is below a tolerance threshold (10^{-4}), stop as $(r^- + r^+)/2$ is an equilibrium.
10. If not, update r grid to $[r^-, r^+]$ and repeat steps 2-8 until convergence.

Two issues emerge. First, solving for optimal conditional consumption and conditional value functions in a model with both discrete and continuous choice variables is harder than traditional pure discrete choice problems. The value functions in equation (8) may not be concave, which affects optimal savings rules even in the presence of extreme value shocks which allow for migration choices to be probabilistic (Iskhakov et al. 2017). In my case, this is likely qualitatively important as value functions differ greatly across locations and constraints on borrowing are frequently biding. The results from Iskhakov et al. (2017) are validated in that the taste shock framework in my setting serves the dual purpose of avoiding issues with degenerate distributions for policy functions over discrete choices of location and smooths value functions more generally. However, in my setting accurately approximating the nonlinearities in policy functions governing migration due to borrowing constraints is critical for the numerical results to correctly account for who stays and leaves.

My difficulties instead emerge with needing to ensure both that my numerical solution captures the nonlinearities in savings policies and accommodates a fine grid for asset holdings despite the large state space. Each node in a traditional asset grid for value function iteration increases the number of values that need to be approximated by 308. Because of the

large dispersion in productivity levels across countries, the asset grid should contain many nodes near $a = 0$ to ensure I capture the concavity in the savings behavior of low-income agents. This requirement for a large number of nodes quickly renders using the benchmark VFI approach where interpolated value functions and numerical differentiation are used for selecting optimal savings policies computationally infeasible. Iskhakov et al. (2017) shows that the endogenous grid methods first proposed in Carroll (2006) improves performance substantially in this dynamic discrete choice setting. Unfortunately I have not had sufficient time during my Ph.D. program to implement this method prior to the job market starting. I instead opt to use a discretized asset grid that allows the inner optimization problem in (9) to be solved using a single “max” operation. As pointed out by Iskhakov et al. (2017), this can produce issues when value functions have kink points or the grid used is sparse. This is especially important in my setting if the grid is too coarse in regions where agents seek to build sufficient wealth to migrate. Further work on my part is needed to ensure the numerical solutions I find are not resulting in large approximation errors.

The second issue is the potential for multiplicity of equilibria even with numerically accurate approximations of value and policy functions in hand. Walsh and Young (2024) show the existence of multiple equilibria for a large set of parameterizations of Aiyagari economies. I further cannot readily apply the comparative static results for large economies from Acemoglu and Jensen (2015) as the extreme value shocks are not drawn from a bounded support. While the risk aversion coefficient with log utility and depreciation value δ I select lie within the parameter space where Walsh and Young (2024) do not find multiple equilibria, it is (in theory) possible that multiple equilibria can exist holding a given interest rate fixed and that along transition paths the results are highly sensitive to the equilibrium which is selected initially.

This form of multiplicity holding interest rates constant may occur, for instance, if there is not a unique invariant measure of agents across locations given a fixed interest rate r which induces an aggregate savings level and effective labor supply such that capital supply is equal to demand. This would be the case if the transition function induced by $\mathbb{E}[\hat{V}(\hat{x}, \hat{d})|r]$ does not satisfy the monotone mixing condition in Hopenhayn and Prescott (1992). Evidence for this form of multiplicity would be hysteresis in the simulated steady-state of the model; the distribution that is produced after a large number of simulated periods would depend on how the model is initialized in terms of agents’ locations and asset holdings. I do not find evidence for this when solving the model numerically. In non-technical terms, it appears that with a long enough sequence of good shocks, agents in the poorest locations do eventually leave and move up in the wealth and location distribution such that the mixing conditions are satisfied. However, I cannot guarantee this is true generally as opposed to being an

object of numerical approximation error.

G Venezuela and Colombia

This appendix serves as an external validation exercise testing for how well a calibrated version of the model can match historical migration dynamics that have been driven by large productivity shocks. As referenced in Section 6, outside of the effects of violent conflict the largest recent historical population change at the national level is the case of Venezuela after Hugo Chavez’s death in 2013. The blue lines in the left and right panels of Figure G.1 show the population and total factor productivity levels in Venezuela between 2000 and 2019 as-recorded in the Penn World Tables version 9.1 (Feenstra, Inklaar, and Timmer 2015). In March of 2013, the then-leader of Venezuela Hugo Chavez passed away. The country subsequently experienced a period of hyperinflation that coincided with a collapse in output and productivity. Between 2013 and 2019, measured productivity in Venezuela fell by 90 percent.

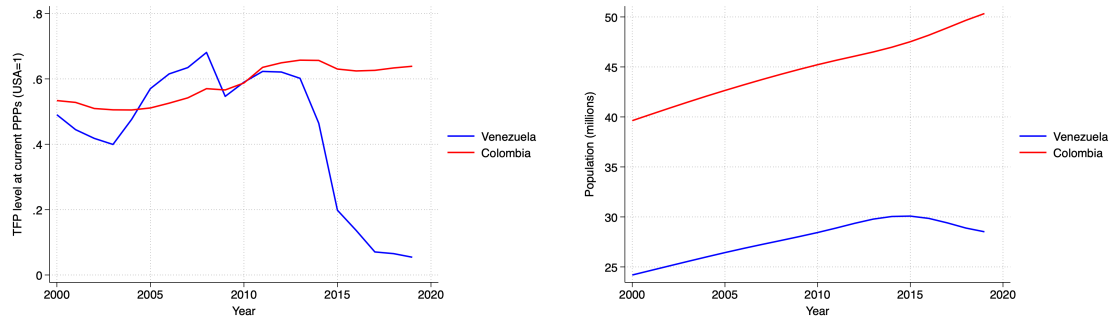


Figure G.1: TFP and Population Levels in Colombia and Venezuela around 2013

Venezuela’s unprecedented collapse in productivity during the 2010s was accompanied by a visible decline in its population, which fell from a peak of over 30 million people in 2015 to 28.5 million in 2019 (the latest year with data in Feenstra, Inklaar, and Timmer 2015). As shown in the blue line in the right panel of Figure G.1, this decline was substantial enough to offset population growth from before 2014. Assuming this decline was driven entirely by Venezuelan emigration, a simple non-parametric extrapolation of pre-2014 trends implies that the Venezuelan population in 2019 is approximately 3.6 million people smaller than the counterfactual trend, as shown in Figure G.2.

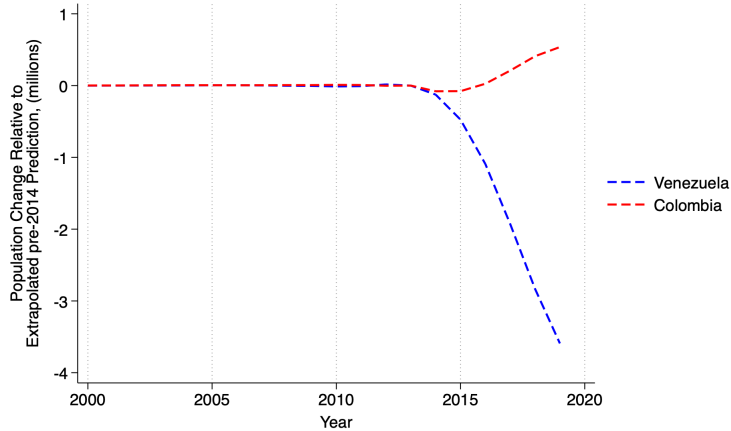


Figure G.2: Deviations from Pre-2014 Trends

A substantial share of Venezuelan emigrants migrated to Colombia. The red line in the right hand panel of Figure G.1 shows Colombia's population during the 2000-19 interval; after 2014 there is a small uptick in the population growth rate, likely driven by Venezuelan emigres. Performing a similar exercise of extrapolation for Colombia suggests that its population in 2019 was 0.5 million people higher than expectations under pre-2014 trends, as shown by the dashed red line in Figure G.2. In contrast with the uptick in population growth, during the 2014-19 period Colombia's total factor productivity was relatively stable at round 60 percent of U.S. levels.

Given the unexpected severity of the decline in Venezuelan economic conditions after 2013, I argue this setting provides a case study for testing the extent to which model parameters must be strained to match realized changes in population levels in the data. As the model is designed to examine transitions between steady-states, this requires from the outset assuming that both (1) prior to the onset of economic crises in Venezuela, both countries can be well-approximated by a stationary equilibrium and (2) the latest year of data I see is a steady-state. The former is due to the inability to solve Aiyagari models globally (ie, for non-stationary solutions), and the latter is a product of a lack of post-2019 observations that may better represent the eventual steady state between the two countries. As such, my case study environment is the effects of falling productivity in Venezuela between 2014 and 2019 on relative population levels in Venezuela and Colombia.

G.1 Initial Equilibrium

First, through the lens of the model prior to 2014, the two regions (Venezuela and Colombia) begin in a stationary recursive competitive equilibrium. This requires choosing an initial

set of population shares and productivity levels to calibrate the model. To simplify this process I abstract from population growth entirely and instead target equilibrium population shares – the share of the combined population of both countries residing in each country. In 2013, approximately 39% of the combined population across the two countries lived in Venezuela.

To force the population shares in the initial stationary equilibrium to coincide with the actual shares, I shut down the migration channel. In the model, this can be achieved by setting the off-diagonal elements of the migration cost matrix to a large positive value. This allows me to exactly match the modeled equilibrium population share to the observed values in the data from 2013. Table G.1 shows the targeted initial population moments, their modeled analogues, and the level of arbitrarily high migration costs I use that precludes migration entirely. I set initial TFP levels to their 2000-2013 averages in each country.

Table G.1: Initial Parameters for Venezuela-Colombia Case Study

Parameter	Col	Vez	Source
Target Moments			
2013 Population Shares	0.61	0.39	Feenstra, Inklaar, and Timmer 2015
Initial Parameters			
$m_{\text{Col} \rightarrow \text{Vez}}$	∞	-	-
$m_{\text{Vez} \rightarrow \text{Col}}$	∞	-	-
Initial Productivity A_{pre}	0.44	0.43	Feenstra, Inklaar, and Timmer 2015

The deep parameters governing production and preferences are shown at the bottom of Table G.1 and are set at relatively standard values for a model period of one year. Parameters governing preferences are identical to those in the main text. The initial modeled equilibrium matches the population shares by construction. The equilibrium real interest rate is 1.45%. I set the bound on borrowing as 0.1, a value slightly more restrictive than the natural borrowing limit for the worst-hit agents in Venezuela in the post-shock equilibrium.

G.2 Modeling post-2013 Venezuela

In 2014, all agents in the model learn that TFP in Venezuela will fall precipitously in the next six years. The agents learn both the new long-run equilibrium level for Venezuelan

TFP (about 0.05 percent of that of the U.S. in 2019) as well as the entire path of TFP along the transition in years 2014-2018. Through the lens of my model, this requires assuming that both the rapid decline in Venezuelan productivity was unexpected prior to 2014, and after 2014 agents knew with certainty both the forthcoming downward trajectory as well as where the bottom would be in 2019. The idealized version of these assumptions is unlikely to hold; the hyperinflation was to some degree expected before 2014, and it is unlikely agents in 2014 knew the extent of the decline in output that was forthcoming.²⁶

Finally, I impose the two-region aspect of the model on the data. Adding more potential absorbing countries for Venezuelan emigrants adds (exponentially) more free parameters with which to fit the post-crash population level in Venezuela in 2019, and as such in my view weakens the credibility of any resulting values of the migration cost matrix. Unlike in reality where Venezuelan emigres could (and did) choose from a set of destinations, the model imposes that all agents leaving Venezuela are doing so to leave Colombia. As such, the modeled Colombia serves more-generally as an absorbing location to see what change in parameters governing costs replicate observed emigration. While I cannot track the final destinations for the population of Venezuelan emigrants, a cursory examination of Figure G.2 suggests this is unlikely to hold in reality - other countries likely absorbed a substantial share of Venezuelan emigrants.²⁷

Table G.2: Model Parameters in New Steady-State

Outside Parameters	Col	Vez	Source
New Productivity A_{post}	0.53	0.02	Penn World Tables
<hr/>			
Target Moments			
<hr/>			
Population Share in 2019	0.65	0.35	Penn World Tables
<hr/>			
Calibrated Parameters			
<hr/>			
m Col → Vez	-0.59	-	Simulated Moments
m Vez → Col	0	-	Simulated Moments
<hr/>			

²⁶In a gross abuse of anecdotal data, I had a Venezuelan student join my high school graduating class in 2011 because her family left the country for economic reasons.

²⁷In favor of the model, Figure G.2 may also underestimate the extent to which Colombia absorbed Venezuelan migrants as they may have avoided full enumeration by statistical agencies in 2019, the last year for which I have data.

Table G.2 shows the parameters governing the new long-run steady state in the model. Long-run productivity rises by about 15% in Colombia while falling by 90 percent in Venezuela. I use the method of moments to find bilateral migration costs that result in a new equilibrium population share for Venezuela that matches the 35 percent of the combined population we see in the data as of 2019. The calibrated bilateral cost for leaving Venezuela is roughly zero, while the cost is a subsidy of -0.59 in the case of emigration from Colombia.

In the new steady state, where TFP in Venezuela has collapsed and migration is no longer prohibited the equilibrium interest rate falls to 1.41%. Comparing these to migration costs, the calibration process uses a subsidy equal to about three quarters of annual Colombian wages to induce a sufficient share of departures in equilibrium to balance out the share of emigrating Venezuelans.

G.3 Modeled Transition Path

The transition period I consider is the years 2014-2019 in the data for the population shares and productivity levels in Venezuela and Colombia. Time series for the TFP for Venezuela and Colombia are taken as evolving exogenously during these periods and are set to match exactly the realization in Figure G.1. Productivity levels in all subsequent modeled years (as the model converges to the new stationary equilibrium) are set equal to those in 2019 shown in Table G.2.

Figure G.3 displays time series for the shares of combined population in Colombia and Venezuela in data between 2014-19 as well their modeled counterparts. Solid lines show the dynamics produced by the model transition path while the dashed lines are values taken from the data (labeled “data” in the figure). “Time since Shock” measures the number of years elapsed since 2014. Prior to time zero, both the data are fixed at 2013 values while the model analogues set at the population shares in the initial stationary equilibrium. Finally, data years after 2019 are also set to 2019 levels. The model overshoots the pace of net emigration from Venezuela in response to the initial shocks; the modeled population share in Venezuela always lies below the actual levels in Figure G.3 after time zero. While this may be driven by misspecification, I believe this is also driven in part by the certainty of agents in the model with regard to the post-2013 TFP trajectory (as opposed to the uncertainty that was likely present in Venezuela at the time of Chavez’s death).

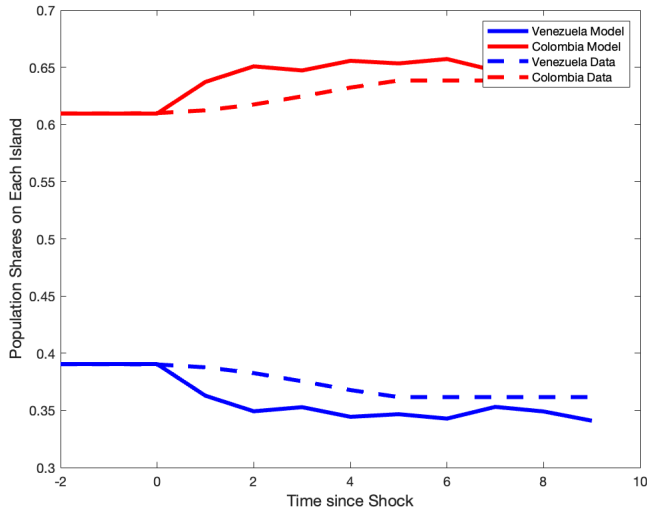


Figure G.3: Modeled and Observed Population Shares in Colombia and Venezuela after 2013

Figure G.4 displays the path of interest rates as well as the associated capital market dynamics during the full transition in which the economy moves towards its steady state. Rates crash in the second and third years of the transition path as the effective labor supply falls a huge amount due to the rapid productivity losses in Venezuela.²⁸ Agents actually increase savings on net in the first period in order to smooth consumption, before drawing the aggregate capital stock down to its new (lower) steady state. The economy reaches the new steady state only after about 50 years, leading the short-run modeled population shares during the transition to overshoot the 2019 equilibrium levels in Figure G.3.

²⁸Rates rise above pre-shock equilibrium levels in the initial year as Colombia's TFP in 2015 begins a bit higher than its 2000-13 average level.

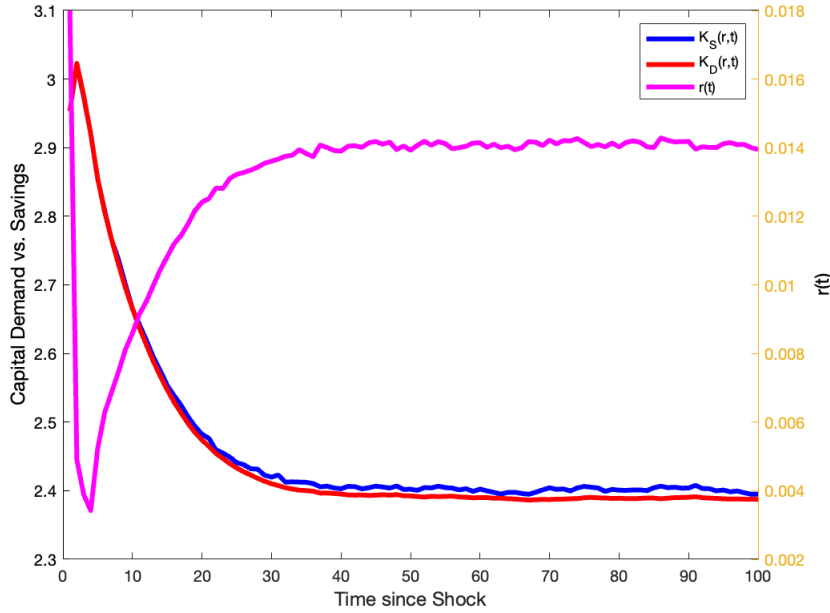


Figure G.4: Convergence to New Steady State

H Solving for Transition Paths

H.1 Solution Algorithm

This appendix provides the details of how to solve for the value and policy functions along a transition path for the model in Section 3 where local fundamental productivity levels change over time. On the transition path, the agent's recursive problem becomes

$$\hat{V}_t(\hat{a}_t, s_t, i_t, \{\lambda_t(j)\}_{j=1}^N) = \max_j \left\{ \max_{\hat{a}_{t+1}} \left\{ u(\hat{c}_t) + \lambda_t(j) + \beta \mathbb{E}[\hat{V}_{t+1}(\hat{a}_{t+1}, s_{t+1}, j_{t+1}, \{\lambda_{t+1}(k)\}_{k=1}^N)] \right\} \right\} \quad (\text{H.1})$$

$$\text{s.t. } (1 + r_t)\hat{a}_t + \hat{w}_{i,t}s_t = \gamma \hat{a}_{t+1} + \hat{c}_t + \hat{m}(i, j)$$

The key difference along the transition path from the stationary equilibrium is the value functions retain their time indices as-defined in in Equation (8). This stems from the fact that the economy is no longer on a balanced growth path; relative wages and interest rates change over time due to the non-stationarity of productivity growth across locations. The objects $\mathbb{E}[\hat{V}_{t+1}(\hat{x}_t, d_t)]$ now solve the functional equation:

$$\mathbb{E}\left[\hat{V}_{t+1}(\hat{x}_t, \hat{d}_t)\right] = \sum_{s' \in \ell, h} \Pi_{ss'} \ln \left(\sum_{k_{t+1}} \exp \left(\max_{\hat{a}_{t+2}} \left\{ u_{t+1}(\hat{x}_{t+1}, d_{t+1}) + \beta \mathbb{E}\left[\hat{V}_{t+2}(x_{t+1}, \hat{d}_{t+1})\right]\right\} \right) \right) \quad (\text{H.2})$$

which like in the non-stationary definition in equation (9) of the main text has time indices on all arguments. The algorithm proceeds as follows:

1. Guess a time T at which the economy has settled into a new stationary equilibrium after the productivity shocks from climate change have been realized.
2. Solve for the initial SCRE, denoted with subscript zero, comprised of $\hat{\Omega}_0(\hat{x}), \hat{V}_0, r_0, \{\hat{w}_0\}, g_0, \pi_0$ under fundamental productivity levels \bar{A}_j .
3. Solve for the new SCRE $\hat{\Omega}_\infty(\hat{x}), \mathbb{E}[\hat{V}_\infty], r_\infty, \{\hat{w}_\infty\}, g_\infty, \pi_\infty$ that is induced by the fundamental productivity levels under fully-realized climate change, \tilde{A}_j .
4. Assume that at time T , the economy along the transition path reaches the new SCRE such that for all times $t \geq T$ we have

$$\mathbb{E}[\hat{V}_{t \geq T}(\hat{x}, \hat{d})] = \mathbb{E}[\hat{V}_\infty(\hat{x}, \hat{d})]$$

and all other equilibrium objects $\pi, \hat{w}, r, g(\hat{x}, j')$ are stationary.

5. Guess a sequence of labor $\{\{N_{i,t}^D\}_{i=1}^N\}_1^{T-1}$ and capital $\{K_t^D\}_1^{T-1}$ demand.
6. Use reverse induction to solve for the series $\{\mathbb{E}[\hat{V}_t]\}_{t=1}^{T-1}$ induced by the guess of aggregate variables along with the sequence of changes in fundamental productivity levels along the transition path
7. Simulate a large number of agents along the transition path and solve for the resulting values of labor supplied $\{\{N_{i,t}^S\}_{i=1}^S\}_1^{T-1}$ and $\{K_t^S\}_1^{T-1}$
8. Adjust guesses for $\{\{N_{i,t}^D\}_{i=1}^N\}_1^{T-1}$ and $\{K_t^D\}_1^{T-1}$ until supply and demand coincide
9. Check if the distribution of assets and agents $\hat{\Omega}_T(\hat{x})$ induced by the sequence of decision rules is equal to the time-invariant value $\hat{\Omega}_\infty(\hat{x})$ within tolerance
10. If it is, algorithm has converged, if not, increase T and go to step 3.

H.2 Average Welfare Losses by Wealth Decile



Figure H.1: Average Welfare Change by Initial Wealth Level Decile

I Steady-State Warming and Productivity Changes under RCP8.5

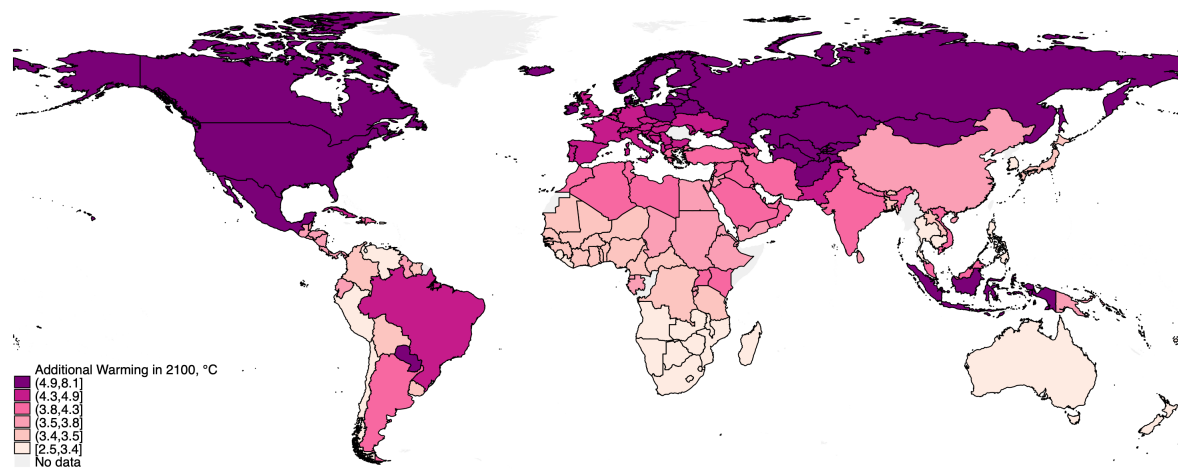


Figure I.1: Forecast Warming in 2100 ($^{\circ}\text{C}$) Under RCP8.5

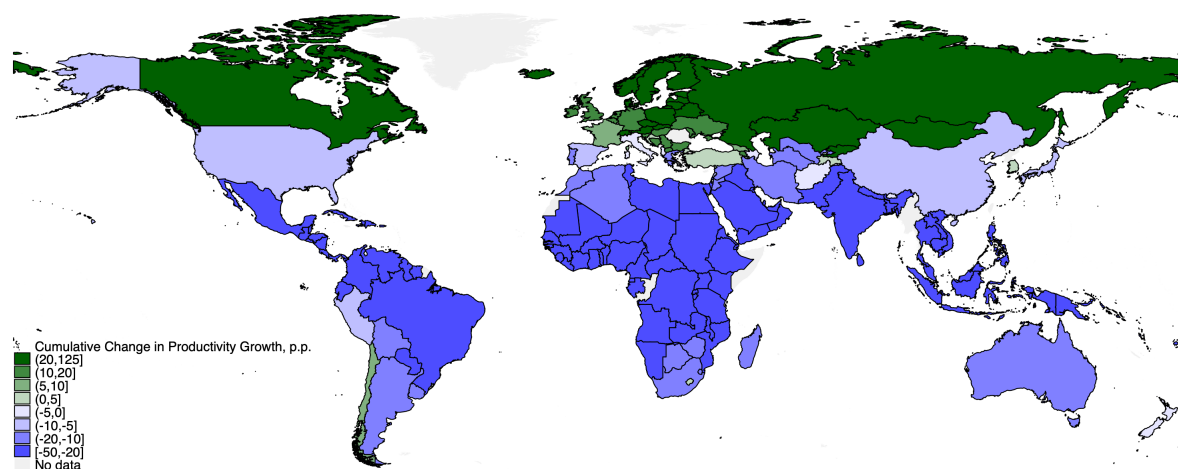


Figure I.2: Cumulative Change in Productivity Growth by 2100 (p.p.) Induced by Climate Change under RCP8.5